

# Opportunistic Relaying in Multicasting over Generalized Shadowed Fading Channels: A PHY Security Analysis

S. M. S. SHAHRIYER<sup>1</sup>, A. S. M. BADRUDDUZA<sup>2</sup>, S. SHABAB<sup>3</sup>, AND M. K. KUNDU<sup>4</sup>

<sup>1,2</sup>Department of Electronics & Telecommunication Engineering, Rajshahi University of Engineering & Technology (RUET), Rajshahi-6204, Bangladesh

<sup>3</sup>Department of Electrical & Electronic Engineering, RUET

<sup>4</sup>Department of Electrical & Computer Engineering, RUET

The secrecy of wireless multicast networks is greatly hampered due to the simultaneous presence of fading and shadowing, which can be enhanced using random attributes of the propagation medium. This work focuses on utilizing those attributes to enhance the physical layer security (PHY security) performance of a dual-hop wireless multicast network over  $\kappa - \mu$  shadowed fading channel under the wiretapping attempts of multiple eavesdroppers. In order to raise the secrecy level, we employ multiple relays with the best relay selection strategy. Performance analysis has been carried out based on the mathematical modeling in terms of closed-form expressions of the probability of non-zero secrecy multicast capacity, secure outage probability for multicasting, and ergodic secrecy multicast capacity. Capitalizing on those expressions, we analyze how the system parameters (i.e. fading, shadowing, the number of antennas, destination receivers, eavesdroppers, and relays) affect the secrecy performance. Our numerical results show that the detrimental impacts due to fading and shadowing can be remarkably mitigated using the well-known opportunistic relaying technique. Moreover, the proposed model unifies secrecy analysis of several classical models, thereby exhibits enormous versatility than the existing works. Finally, all the numerical results are authenticated utilizing Monte-Carlo simulations.

**Keywords:**  $\kappa - \mu$  shadowed fading, opportunistic relaying, physical layer security, secure outage probability, wireless multicasting.

## 1. INTRODUCTION

### A. Background and Related Works

Data carrying radio waves while propagating through communication channels experience several constraints such as diffraction, scattering of waves on the object surface, shadowing, fading, limited bandwidth, and vulnerable nature of the wireless medium, etc. Especially, random shadowing caused by obstacles in the local scenarios or human body exhibits some variations in the interaction pattern of radio wave propagation. Therefore, the aim to build a fortified network not only involves the enhancement of communicating link performance but also the use of optimized protocols in transmitter and receiver circuitry to prevent shadowing and swift variations in multipath propagation conditions.

To understand the effect of dominant and scattered components of the dual shadowing process, authors in [1] derived expressions of probability density function (PDF), cumulative distribution function (CDF), and Moment Generating Function (MGF) of Rician fading envelopes. In [2], authors analyzed outage performance

over compound  $\eta - \mu$  fading-log-normal shadowing radio channels and derived a unique formula for the PDF of  $\eta - \mu$  fading distribution. With a view to unifying all classic fading models, the authors investigated the ergodic capacity (EC) and flexibility [3, 4] of the channel for complex Gaussian random variable. Similarly, a trade-off between mathematical complexity and flexibility was represented in [5] by varying different fading parameters under Rayleigh fading distribution. Optimal rate adaptation (ORA) scheme under composite  $\kappa - \mu$ /Inverse Gamma (I-Gamma) and  $\eta - \mu$ /Inverse Gamma [6] fading models was investigated in [7], where the analysis incorporated expressions of channel capacity (CP) with a view to developing highly attractive wireless communication systems. Authors in [8] studied average symbol error probability (SEP), the CP under ORA, channel inversion with fixed-rate (CIFR), and truncated CIFR under I-Gamma shadowed fading channel. A qualified analysis among Log-Normal, Inverse Gaussian [9], Gamma, and I-Gamma distribution was also depicted. Apart from these fading channels, the  $\kappa - \mu$  shadowed fading channel gained much popularity because of its broad spectrum of flexibility and general characterization. The researchers in [10, 11] proposed a  $\kappa - \mu$  shadowed fading model to improve network quality, capacity, and spectral efficiency taking human body shadowing under consideration. Maximum ratio combining (MRC) and square-law combining schemes over  $\kappa - \mu$  shadowed fading channel were performed in [12–15] to observe energy detection in wireless communication scenarios. With the interest of investigating the effective rate of the multiple-input multiple-output (MIMO) systems, the authors in [16, 17] performed higher-order statistics analysis and proved that the properties of the considered fading distribution could be approximated by Gamma distribution. Multiplicative shadowing was investigated in [18, 19], where the authors showed the superiority of  $\kappa - \mu$  / Gamma composite fading model over  $\kappa - \mu$  / log-normal line-of-sight (LOS) shadowed fading model in an indoor off-body communication system.

Presently, the need for security enhancement between communicating devices in wireless medium has become a major concern. To compensate for the consequences due to several hindrances such as shadowing, fading, wiretapping, and a notable amount of researches have been introduced to build reliable wireless networks to make it impossible for any eavesdropper to decode any information from the communicating network. Wyner's classic wiretap structure is known as the leading model which recapitulates the importance of security enhancement over different fading channels. Among them, shadowed fading distribution is more admissible for being amenable than any other modern fading model and its vast span of propagation conditions. In an extension of this fact, outage performance over log-normal shadowed Rayleigh fading channel was analyzed [20, 21], where the authors prosecuted the Gaussian-Hermite integration approach to show that outage performance significantly enhances standard deviations of shadowing. Authors in [22] analyzed the impact of shadowing on numbers of antennas and propagation conditions over secrecy performance deriving several secrecy measures. Free space optical (FSO) links undergoing shadowed Rician and  $\alpha - \mu$  fading in [23] were analyzed to achieve a perfect secrecy level despite severe channel constraints. To get the more generalized picture, security over  $\kappa - \mu$  shadowed fading model at physical layer was examined in [24–26], where authors demonstrated that MIMO system diversity manifests superior performance over MRC and selecting diversity in case of security. Authors in [27, 28] considered  $\kappa - \mu$  shadowed fading channels to observe the effect of correlation and drew a conclusion on the fact that the correlation coefficient works as a propitious parameter in case of improving secrecy performance at a lower signal-to-noise ratio (SNR).

Cooperative relaying is another proficient skill to enhance security in wireless systems [29]. The impact of shadowing is inevitably minimized using the dual-hop network which in turn helps to improve wireless links. A multi-branch-multi-hop cooperative relaying system in the presence of co-channel interferers was considered in [30, 31] over shadowed Nakagami- $m$  channel, where the authors evinced that fading parameter affects the system performance greater than the shadowing parameter. A multiple cooperative relay-based satellite-terrestrial system over non-identical shadowed Rician and Nakagami- $m$  fading channels was studied in [32, 33], where the authors came to a conclusion that EC of the system decreases with increasing relay nodes between satellite and ground users. The best relay selection scheme was employed while analyzing the performance of  $\kappa - \mu$  shadowed fading channel with multiple relays in [34]. The authors examined the expressions of outage probability (OP), EC, and average bit error rate (ABER) to manifest the superiority of multiple relay systems over all other transmission techniques. Performance of a  $\kappa - \mu$  shadowed fading

model with beam-forming and amplify-and-forward (AF) relaying technique was demonstrated in [35, 36]. The author validated the fact that the increment in the number of antennas at the transmitting earth station (ES) provides finer performance compared to the increment in the number of antennas at the receiving ES.

Recently, multicasting has earned much popularity in wireless communication due to its versatile nature to transmit data to multiple destinations accommodating fewer network supplies. Due to this wide acceptance of wireless multicasting, novel researches are underway to enhance the secrecy performance. Physical layer security (PLS) of a multicasting scenario was analyzed in [37] and [38] over quasi-static Rayleigh fading and generalized  $\kappa - \mu$  fading channels, respectively. In both papers, the authors derived the expressions of the probability of non-zero secrecy multicast capacity (PNSMC) and secure outage probability for multicasting (SOPM), though the authors in [38] considered a multiple relay system with the best relay selection scheme. A virtual MIMO antenna array scheme was employed in a multiple relay system in [39, 40], where authors provided a completed description on co-operative spatial multiplexing and derived expressions of SOPM and ergodic secrecy multicast capacity (ESMC). The authors proved that the secrecy performance of a cooperative network completely outweighs that of a direct network.

## B. Motivation and Contribution

According to the aforementioned works, most of the researches was performed to investigate the system's improvement applying numerous methods over various fading channels (i.e. both generalized and multipath). But there are few works that considered the wireless multicasting scenario and even no authors have investigated the impact of shadowing on the secure wireless multicast schemes with opportunistic relaying and multiple eavesdroppers over multipath/generalized shadowed fading channels yet. Motivated from this perspective, this paper represents the mathematical modeling of a secure wireless multicasting scheme over  $\kappa - \mu$  shadowed fading channels with an opportunistic relaying technique. Here a single sender communicates with a set of destination receivers via a set of co-operative relays in the existence of a set of eavesdroppers.  $\kappa - \mu$  shadowed model assumes random fluctuations of LOS component and also matches well with experimental data of land mobile satellite (LMS) communication channel. Moreover,  $\kappa - \mu$  fading channel is a generalized fading model, and hence a number of classical fading models (e.g., One-sided Gaussian, Nakagami- $m$ , Rayleigh, Rician- $K$ , and shadowed Rician) can be obtained as particular cases of the proposed model. The prime contributions of the authors are as follows:

1. We derive the PDF and CDF of SNRs for multicast and eavesdropper channels by first realizing the PDF of SNRs of each individual hop and then obtaining the PDF of dual-hop SNR with the best relay selection algorithm. To the best of the authors' knowledge, the derived PDF and CDF are absolutely novel and have not been reported yet in any existing literature.
2. We analyze the secrecy performance utilizing novel expressions of some well-known secrecy metrics i.e. PNSMC, SOPM, and ESMC, and quantify the effects of each system parameter (i.e. fading parameters, shadowing, number of receive antennas, relays, destination receivers, and eavesdroppers, etc). In comparison to the previous literature, only the proposed work demonstrates how the detrimental impact of shadowing on secure multicasting can be mitigated employing an opportunistic relaying strategy.
3. Finally, we verify all the numerical results corresponding to the derived expressions of secrecy metrics via Monte-Carlo simulations.

## C. Paper Organisation

The organization of this paper is summarized as follows: Section 2 discusses the proposed system model and problem formulation. The derivations of the expressions of secrecy metrics i.e. PNSMC, SOPM, and ESMC are demonstrated in Section 3. Section 4 provides the numerical results analysis. Finally, the conclusion of this work is illustrated in section 5.

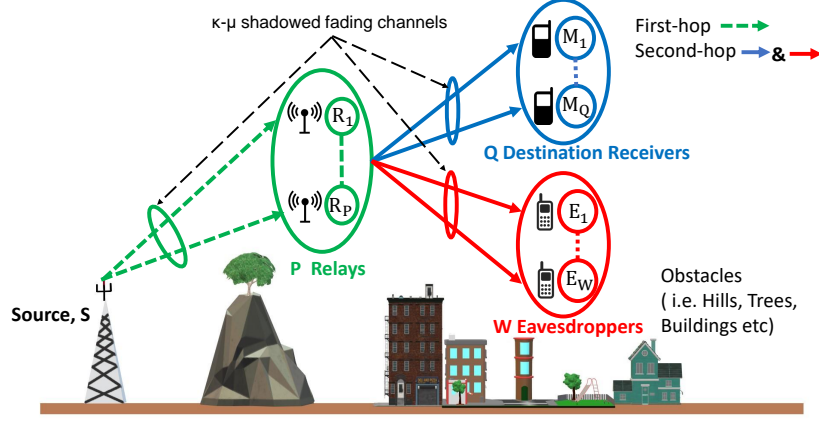


Fig. 1. Proposed system model.

## 2. SYSTEM MODEL AND PROBLEM FORMULATION

A secure wireless multicast network is shown in Fig.1, where a source,  $S$  with a single antenna sends secret information to a set of  $Q$  destination receivers via  $P$  relays. A set of  $W$  eavesdroppers are also present in that network which is intended to decipher the secret messages. Each relay has a single antenna while each destination receiver and each eavesdropper are equipped with  $G_Q$  and  $G_W$  antennas, respectively. In this particular communication scenario, we assume similar to [38] that the distances of  $Q$  and  $W$  from  $S$  are too large and due to masking effect, and severe shadowing there are no direct communication paths between  $S$  to  $Q$  as well as  $S$  to  $W$ . Hence the only communication path that exists is through the relay. The overall process is performed in two phases. In the first-hop,  $S$  sends messages to the relay. Then, in the second-hop, desired messages are received by the destination receivers from the best relay only. Meanwhile, at the same time slot, the eavesdroppers also try to steal information from a best relay.

The direct channel coefficients for  $S$  to  $a$ th ( $a = 1, 2, 3, \dots, P$ ) relay link is  $f_{s,a} \in \mathcal{C}^{1 \times 1}$ , for  $a$ th relay to  $b$ th ( $b = 1, 2, 3, \dots, Q$ ) destination receiver link is  $\mathbf{g}_{a,b} \in \mathcal{C}^{G_Q \times 1}$  (i.e.  $\mathbf{g}_{ab} = [g_{1ab} \ g_{2ab} \ g_{3ab} \ \dots \ g_{G_Q ab}]^T$ ) and for  $a$ th relay to  $c$ th ( $c = 1, 2, 3, \dots, W$ ) eavesdropper link is  $\mathbf{h}_{a,c} \in \mathcal{C}^{G_W \times 1}$  (i.e.  $\mathbf{h}_{ac} = [h_{1ac} \ h_{2ac} \ h_{3ac} \ \dots \ h_{G_W ac}]^T$ ).

In the first-hop, the received signal at  $a$ th relay is expressed as

$$y_{s,a} = f_{s,a}x + z_a, \quad (1)$$

where  $x \sim \tilde{\mathcal{N}}(0, T_s)$  is the transmitted message signal from  $S$ ,  $T_s$  is the transmit power,  $z_a \sim \tilde{\mathcal{N}}(0, N_a)$  indicates the additive white gaussian noise (AWGN) imposed on  $a$ th relay with noise power  $N_a$ .

In the second-hop, the received signal of the  $a$ th best relay will be forwarded to the receivers. Hence, the received signals at the  $b$ th receiver is denoted as

$$\begin{aligned} \mathbf{y}_{a,b} &= \mathbf{g}_{a,b}y_{s,a} + \mathbf{j}_b = \mathbf{g}_{a,b}(f_{s,a}x + z_a) + \mathbf{j}_b \\ &= \mathbf{d}_{ab}x + \mathbf{u}_b, \end{aligned} \quad (2)$$

whereas the received signal at  $c$ th eavesdropper can be written as

$$\begin{aligned} \mathbf{y}_{a,c} &= \mathbf{h}_{a,c}y_{s,a} + \mathbf{k}_c = \mathbf{h}_{a,c}(f_{s,a}x + z_a) + \mathbf{k}_c \\ &= \mathbf{d}_{ac}x + \mathbf{v}_c. \end{aligned} \quad (3)$$

Here,  $\mathbf{u}_b \triangleq \mathbf{g}_{a,b}z_a + \mathbf{j}_b$ ,  $\mathbf{v}_c \triangleq \mathbf{h}_{a,c}z_a + \mathbf{k}_c$ ,  $\mathbf{d}_{a,b} = \mathbf{g}_{a,b}f_{s,a}$ ,  $\mathbf{d}_{a,c} = \mathbf{h}_{a,c}f_{s,a}$ ,  $\mathbf{j}_b \sim \tilde{\mathcal{N}}(0, N_b \mathbf{I}_{G_Q})$  and  $\mathbf{k}_c \sim \tilde{\mathcal{N}}(0, N_c \mathbf{I}_{G_W})$  symbolize the noises imposed on the  $b$ th receiver and  $c$ th eavesdropper,  $N_b$  and  $N_c$  represent noise powers, and  $\mathbf{I}_G(\cdot)$  is the identity matrix of order  $G \times G$ .

We assume all the channels between source to relays ( $S \rightarrow P$  links), relays to destination receivers ( $P \rightarrow Q$  links), and relays to eavesdroppers ( $P \rightarrow W$  links) undergo independent and identically distributed (i.i.d.)

$\kappa - \mu$  shadowed fading i.e. all the LOS components are subjected to shadowing. This channel is widely used to model land mobile satellite communication systems. Moreover, this model exhibits extreme versatility since a wide number of multipath/generalized fading models can be obtained as special cases from this particular model as shown in Table 1.

**Table 1.** Special Cases of  $\kappa - \mu$  shadowed fading channel [13].

Fading Channels	$\kappa - \mu$ Shadowed Fading Parameters		
	$\kappa_b = \kappa_c = \kappa_a$	$\mu_b = \mu_c = \mu_a$	$m_b = m_c = m_a$
One Sided Gaussian	0	0.5	$\infty$
Rayleigh	0	1	$\infty$
Nakagami- $m$	0	$m$	$\infty$
Shadowed Rician	$K$	1	$m$
Rician- $K$	$K$	1	$\infty$

### A. Channel Model

The instantaneous SNRs of  $S \rightarrow P$ ,  $P \rightarrow Q$  and  $P \rightarrow W$  links are respectively given by  $\theta_{s,a} = \frac{T_s}{N_a} \|f_{s,a}\|^2$ ,  $\theta_{a,b} = \frac{P_a}{N_b} \|\mathbf{g}_{a,b}\|^2$ , and  $\theta_{a,c} = \frac{P_a}{N_c} \|\mathbf{h}_{a,c}\|^2$ , where  $P_a$  is the transmit signal power from the relay. The PDF of respective SNRs are shown below.

#### A.1. PDF of $\theta_{s,a}$

The PDF of  $\theta_{s,a}$  is given by [eq. 1, 41]

$$f_{s,a}(\theta) = \alpha_1 e^{-\mathcal{A}_2 \theta} \theta^{\mu_a - 1} {}_1F_1(m_a, \mu_a; \alpha_3 \theta), \quad (4)$$

where  $\alpha_1 = \frac{\mu_a^{\mu_a} m_a^{m_a} (1 + \kappa_a)^{\mu_a}}{\Gamma(\mu_a) \bar{\theta}_{sa}^{\mu_a} (\mu_a \kappa_a + m_a)^{m_a}}$ ,  $\mathcal{A}_2 = \frac{\mu_a (1 + \kappa_a)}{\bar{\theta}_{sa}}$ ,  $\alpha_3 = \frac{\mu_a^2 \kappa_a (1 + \kappa_a)}{(\mu_a \kappa_a + m_a) \bar{\theta}_{sa}}$ , the average SNR of  $S \rightarrow P$  link channel is  $\bar{\theta}_{sa}$ ,  $\kappa_a$  is the ratio of the powers between dominant and scattered components,  $\mu_a$  is the number of clusters,  $m_a$  is the Nakagami- $m$  faded shadowing component and  ${}_1F_1(\cdot, \cdot; \cdot)$  is the confluent hyper-geometric function which can be expressed as  ${}_1F_1(x_1, y_1; z_1) = \frac{\Gamma(y_1)}{\Gamma(x_1)} \sum_{d_1=0}^{\infty} \frac{\Gamma(x_1 + d_1) z_1^{d_1}}{\Gamma(y_1 + d_1) d_1!}$  [eq. 13, 42]. Hence, finally  $f_{s,a}(\theta)$  can be written as

$$f_{s,a}(\theta) = \sum_{e_1=0}^{\infty} \mathcal{A}_1 e^{-\mathcal{A}_2 \theta} \theta^{\mathcal{A}_3}, \quad (5)$$

where  $\mathcal{A}_1 = \alpha_1 \alpha_{e_1}$ ,  $\alpha_{e_1} = \frac{\Gamma(\mu_a) \Gamma(m_a + e_1) \alpha_3^{e_1}}{\Gamma(m_a) \Gamma(\mu_a + e_1) e_1!}$ , and  $\mathcal{A}_3 = \mu_a - 1 + e_1$ .

#### A.2. PDF of $\theta_{a,b}$

Similar to Eq. (5), PDF of  $\theta_{a,b}$  can be written as [eq. 1, 41]

$$f_{a,b}(\theta) = \sum_{e_2=0}^{\infty} \mathcal{B}_1 e^{-\mathcal{B}_2 \theta} \theta^{\mathcal{B}_3}, \quad (6)$$

where  $\mathcal{B}_1 = \beta_1 \beta_{e_2} \beta_1 = \frac{(G_Q \mu_b)^{G_Q \mu_b} (G_Q m_b)^{G_Q m_b} (1 + \kappa_b)^{G_Q \mu_b}}{\Gamma(G_Q \mu_b) (\bar{\theta}_{ab})^{G_Q \mu_b} (G_Q \mu_b \kappa_b + G_Q m_b)^{G_Q m_b}}$ ,  $\beta_{e_2} = \frac{\Gamma(G_Q \mu_b) \Gamma(G_Q m_b + e_2) \beta_2^{e_2}}{\Gamma(G_Q m_b) \Gamma(G_Q \mu_b + e_2) e_2!}$ ,  $\beta_2 = \frac{G_Q^2 \mu_b^2 \kappa_b (1 + \kappa_b)}{(G_Q \mu_b \kappa_b + G_Q m_b) \bar{\theta}_{ab}}$ ,  $\mathcal{B}_2 = \frac{G_Q \mu_b (1 + \kappa_b)}{\bar{\theta}_{ab}}$ ,  $\mathcal{B}_3 = G_Q \mu_b - 1 + e_2$ , the average SNR of  $P \rightarrow Q$  link channel is  $\bar{\theta}_{ab}$  and shape parameters corresponding to  $P \rightarrow Q$  link are denoted by  $\kappa_b$ ,  $\mu_b$  and  $m_b$ .

### A.3. PDF of $\theta_{a,c}$

The PDF of  $\theta_{a,c}$  can be expressed as [eq. 1, 41]

$$f_{a,c}(\theta) = \sum_{e_3=0}^{\infty} \mathcal{C}_1 e^{-C_2 \theta} \theta^{C_3}, \quad (7)$$

where  $\mathcal{C}_1 = \iota_1 \iota_{e_3} \iota_1 = \frac{(G_W \mu_c)^{G_W \mu_c} (G_W m_c)^{G_W m_c} (1 + \kappa_c)^{G_W \mu_c}}{\Gamma(G_W \mu_c) (\bar{\theta}_{ac})^{G_W \mu_c} (G_W \mu_c \kappa_c + G_W m_c)^{G_W m_c}}$ ,  $\iota_{e_3} = \frac{\Gamma(G_W \mu_c) \Gamma(G_W m_c + e_3) \iota_2^{e_3}}{\Gamma(G_W m_c) \Gamma(G_W \mu_c + e_3) e_3!}$ ,  $\iota_2 = \frac{G_W^2 \mu_c^2 \kappa_c (1 + \kappa_c)}{(G_W \mu_c \kappa_c + G_W m_c) \bar{\theta}_{ac}}$ ,  $\mathcal{C}_2 = \frac{G_W \mu_c (1 + \kappa_c)}{\bar{\theta}_{ac}}$ ,  $\mathcal{C}_3 = G_W \mu_c - 1 + e_3$ , the average SNR of  $P \rightarrow W$  link is  $\bar{\theta}_{ac}$  and  $\kappa_c$ ,  $\mu_c$  and  $m_c$  symbolize the shape parameters corresponding to  $P \rightarrow W$  link.

### B. PDFs of Dual-hop SNRs

Denoting SNRs of  $S \rightarrow Q$  and  $S \rightarrow W$  links by  $\theta_{s,b}$  and  $\theta_{s,c}$ , respectively, the PDFs of  $\theta_{s,b}$  and  $\theta_{s,c}$  are defined as [43]

$$f_{s,b}(\theta) = \frac{dF_{s,b}(\theta)}{d\theta}, \quad (8)$$

$$f_{s,c}(\theta) = \frac{dF_{s,c}(\theta)}{d\theta}, \quad (9)$$

where  $F_{s,b}(\theta)$ , and  $F_{s,c}(\theta)$  express the CDFs of  $\theta_{s,b}$ , and  $\theta_{s,c}$ . The CDF of  $\theta_{s,b}$  is defined as [eq. 12, 44], [45]

$$F_{s,b}(\theta) = 1 - Pr(\theta_{s,a} > \theta_{s,b}) Pr(\theta_{a,b} > \theta_{s,b}), \quad (10)$$

where  $Pr(\theta_{s,a} > \theta_{s,b})$  and  $Pr(\theta_{a,b} > \theta_{s,b})$  are the complementary cumulative distribution functions (CCDFs) of  $\theta_{s,a}$  and  $\theta_{a,b}$ , and the CCDFs are respectively defined as [eq. 9.368, 46]

$$Pr(\theta_{s,a} > \theta_{s,b}) = \int_{\theta_{s,b}}^{\infty} f_{s,a}(\theta) d\theta, \quad (11)$$

$$Pr(\theta_{a,b} > \theta_{s,b}) = \int_{\theta_{s,b}}^{\infty} f_{a,b}(\theta) d\theta. \quad (12)$$

Substituting Eq. (5) into Eq. (11) and executing integration using the following identity of [eq. 3.351.2, 47], we get

$$Pr(\theta_{s,a} > \theta_{s,b}) = \sum_{e_1=0}^{\infty} \mathcal{A}_1 \mathcal{A}_2^{-\mu_a - e_1} \Gamma(\mu_a + e_1, \mathcal{A}_2 \theta_{s,b}). \quad (13)$$

Further, substituting Eq. (6) into Eq. (12) and performing integration, we have

$$Pr(\theta_{a,b} > \theta_{s,b}) = \sum_{e_2=0}^{\infty} \mathcal{B}_1 \mathcal{B}_2^{-G_Q \mu_b - e_2} \Gamma(G_Q \mu_b + e_2, \mathcal{B}_2 \theta_{s,b}). \quad (14)$$

Deploying Eq. (13) and Eq. (14) into Eq. (10), the CDF of  $\theta_{s,b}$  is obtained as

$$F_{s,b}(\theta) = 1 - \sum_{e_2=0}^{\infty} \sum_{e_1=0}^{\infty} \Theta_{e_2} \Gamma(\mu_a + e_1, \mathcal{A}_2 \theta) \times \Gamma(G_Q \mu_b + e_2, \mathcal{B}_2 \theta), \quad (15)$$

where  $\Theta_{e_2} = \mathcal{A}_1 \mathcal{B}_1 \mathcal{A}_2^{-\mu_a - e_1} \mathcal{B}_2^{-G_Q \mu_b - e_2}$ . Now, substituting Eq. (15) into Eq. (8) and performing differentiation with respect to  $\theta_{s,b}$ , the PDF of  $\theta_{s,b}$  is found as

$$f_{s,b}(\theta) = \sum_{s_2=0}^{\infty} \sum_{e_4=0}^{\infty} \frac{\Theta_{e_4} \theta^{\mu_a + s_2 - 1}}{e^{\mathcal{A}_2 \theta}} \Gamma(G_Q \mu_b + e_4, \mathcal{B}_2 \theta) + \sum_{s_3=0}^{\infty} \sum_{e_5=0}^{\infty} \frac{\Theta_{e_5} \theta^{G_Q \mu_b + e_5 - 1}}{e^{\mathcal{B}_2 \theta}} \Gamma(\mu_a + s_3, \mathcal{A}_2 \theta), \quad (16)$$



where  $\Theta_{e_4} = \mathcal{A}_1 \mathcal{B}_1 \mathcal{A}_2^{-\mu_a - s_2} \mathcal{B}_2^{-G_Q \mu_b - e_4}$  and  $\Theta_{e_5} = \mathcal{A}_1 \mathcal{B}_1 \mathcal{A}_2^{-\mu_a - s_3} \mathcal{B}_2^{-G_Q \mu_b - e_5}$ . Similarly, the CDF of  $\theta_{s,c}$  can be obtained as

$$F_{s,c}(\theta) = 1 - \sum_{e_3=0}^{\infty} \sum_{e_1=0}^{\infty} \Theta_{e_3} \Gamma(\mu_a + e_1, \mathcal{A}_2 \theta) \times \Gamma(G_W \mu_c + e_3, \mathcal{C}_2 \theta), \quad (17)$$

where  $\Theta_{e_3} = \mathcal{A}_1 \mathcal{C}_1 \mathcal{A}_2^{-\mu_a - e_1} \mathcal{C}_2^{-G_W \mu_c - e_3}$ . Furthermore, replacing Eq. (17) into Eq. (9), the PDF of  $\theta_{s,c}$  is obtained as

$$f_{s,c}(\theta) = \sum_{s_4=0}^{\infty} \sum_{e_6=0}^{\infty} \frac{\Theta_{e_6} \theta^{\mu_a + s_4 - 1}}{e^{\mathcal{A}_2 \theta}} \Gamma(G_W \mu_c + e_6, \mathcal{C}_2 \theta) + \sum_{s_5=0}^{\infty} \sum_{e_7=0}^{\infty} \frac{\Theta_{e_7} \theta^{G_W \mu_c + e_7 - 1}}{e^{\mathcal{C}_2 \theta}} \Gamma(\mu_a + s_5, \mathcal{A}_2 \theta), \quad (18)$$

where  $\Theta_{e_6} = \mathcal{A}_1 \mathcal{C}_1 \mathcal{A}_2^{-\mu_a - s_4} \mathcal{C}_2^{-G_W \mu_c - e_6}$  and  $\Theta_{e_7} = \mathcal{A}_1 \mathcal{C}_1 \mathcal{A}_2^{-\mu_a - s_5} \mathcal{C}_2^{-G_W \mu_c - e_7}$ .

### C. Best Relay Selection

Let  $\theta_b^*$  denote the SNR between best relay and  $b$ th receiver which is expressed as [eq. 8, 48]

$$\theta_b^* = \arg_{a \in \omega}^{\max} \min(\theta_{s,a}, \theta_{a,b}), \quad (19)$$

where  $\omega = 1, 2, \dots, P$  is the relay set. The CDF of  $\theta_b^*$  is demonstrated as

$$F_{*,b}(\theta) = [F_{s,b}(\theta)]^P. \quad (20)$$

Hence, substituting Eq. (15) into Eq. (20), the CDF of  $\theta_b^*$  is derived as

$$F_{*,b}(\theta) = \left[ 1 - \sum_{e_2=0}^{\infty} \sum_{e_1=0}^{\infty} \Theta_{e_2} \Gamma(\mu_a + e_1, \mathcal{A}_2 \theta) \times \Gamma(G_Q \mu_b + e_2, \mathcal{B}_2 \theta) \right]^P. \quad (21)$$

Differentiating Eq. (20) with respect to  $\theta_{s,b}$ , the PDF of  $\theta_b^*$  is obtained as

$$f_{*,b}(\theta) = P f_{s,b}(\theta) [F_{s,b}(\theta)]^{P-1}. \quad (22)$$

Again, deploying Eq. (15) and Eq. (16) into Eq. (22),  $f_{*,b}(\theta)$  is given by

$$\begin{aligned} f_{*,b}(\theta) = P & \left[ \sum_{s_2=0}^{\infty} \sum_{e_4=0}^{\infty} \frac{\Theta_{e_4} \theta^{\mu_a + s_2 - 1}}{e^{\mathcal{A}_2 \theta}} \Gamma(G_Q \mu_b + e_4, \mathcal{B}_2 \theta) + \sum_{s_3=0}^{\infty} \sum_{e_5=0}^{\infty} \frac{\Theta_{e_5} \theta^{G_Q \mu_b + e_5 - 1}}{e^{\mathcal{B}_2 \theta}} \Gamma(\mu_a + s_3, \mathcal{A}_2 \theta) \right] \\ & \times \left[ 1 - \sum_{e_2=0}^{\infty} \sum_{e_1=0}^{\infty} \Theta_{e_2} \Gamma(\mu_a + e_1, \mathcal{A}_2 \theta) \Gamma(G_Q \mu_b + e_2, \mathcal{B}_2 \theta) \right]^{P-1}. \end{aligned} \quad (23)$$

Similar to Eq. (19), the SNR between best relay and  $c$ th eavesdropper denoted by  $\theta_c^*$  is explained as [eq. 8, 48]

$$\theta_c^* = \arg_{a \in \omega}^{\max} \min(\theta_{s,a}, \theta_{a,c}), \quad (24)$$

the CDF of which is given by

$$F_{*,c}(\theta) = [F_{s,c}(\theta)]^P. \quad (25)$$

Substituting Eq. (17) into Eq. (25), the CDF of  $\theta_c^*$  is obtained as

$$F_{*,c}(\theta) = \left[ 1 - \sum_{e_3=0}^{\infty} \sum_{e_1=0}^{\infty} \Theta_{e_3} \Gamma(\mu_a + e_1, \mathcal{A}_2 \theta) \times \Gamma(G_W \mu_c + e_3, \mathcal{C}_2 \theta) \right]^P. \quad (26)$$

Further, differentiating Eq. (25) with respect to  $\theta_{s,c}$ , and substituting Eq. (17) and Eq. (18) into it, the PDF of  $\theta_c^*$  is derived as

$$\begin{aligned} f_{*,c}(\theta) = P & \left[ \sum_{s_4=0}^{\infty} \sum_{e_6=0}^{\infty} \frac{\Theta_{e_6} \theta^{\mu_a + s_4 - 1}}{e^{\mathcal{A}_2 \theta}} \Gamma(G_W \mu_c + e_6, \mathcal{C}_2 \theta) + \sum_{s_5=0}^{\infty} \sum_{e_7=0}^{\infty} \frac{\Theta_{e_7} \theta^{G_W \mu_c + e_7 - 1}}{e^{\mathcal{C}_2 \theta}} \Gamma(\mu_a + s_5, \mathcal{A}_2 \theta) \right] \\ & \times \left[ 1 - \sum_{e_3=0}^{\infty} \sum_{e_1=0}^{\infty} \Theta_{e_3} \Gamma(\mu_a + e_1, \mathcal{A}_2 \theta) \Gamma(G_W \mu_c + e_3, \mathcal{C}_2 \theta) \right]^{P-1}. \end{aligned} \quad (27)$$

#### D. Modeling of Multicast Channels

Note that we consider multiple destination receivers ( $Q$ ) each of which can receive the multicast messages at the same instant. To ascertain a secure communication with each receiver, we demonstrate secrecy analysis considering the worst possible scenario which includes taking into consideration the minimum SNR among all receivers as denoted by  $\theta_{\min} = \min_{1 < b < Q} \theta_b^*$ . Hence, it is clear from this consideration that if the proposed system is capable of protecting multicast information from being eavesdropped for the worst case, then for all other cases (i.e. better than worst case), the system will undoubtedly be secure. Since,  $\theta_1^*, \theta_2^*, \dots, \theta_Q^*$  are all independent, using order statistics, the PDF of  $\theta_{\min}$  can be defined as [eq. 33, 38]

$$f_{\theta_{\min}}(\theta) = Q f_{*,b}(\theta) [1 - F_{*,b}(\theta)]^{Q-1}. \quad (28)$$

Now, substituting Eq. (21) and Eq. (23) into Eq. (28),  $f_{\theta_{\min}}(\theta)$  is obtained as

$$\begin{aligned} f_{\theta_{\min}}(\theta) = PQ & \left[ \sum_{s_2=0}^{\infty} \sum_{e_4=0}^{\infty} \frac{\Theta_{e_4} \theta^{\mu_a + s_2 - 1}}{e^{\mathcal{A}_2 \theta}} \Gamma(G_Q \mu_b + e_4, \mathcal{B}_2 \theta) + \sum_{s_3=0}^{\infty} \sum_{e_5=0}^{\infty} \frac{\Theta_{e_5} \theta^{G_Q \mu_b + e_5 - 1}}{e^{\mathcal{B}_2 \theta}} \Gamma(\mu_a + s_3, \mathcal{A}_2 \theta) \right] \\ & \times \left[ 1 - \sum_{e_2=0}^{\infty} \sum_{e_1=0}^{\infty} \Theta_{e_2} \Gamma(\mu_a + e_1, \mathcal{A}_2 \theta) \Gamma(G_Q \mu_b + e_2, \mathcal{B}_2 \theta) \right]^{P-1} \times \left[ 1 - \left[ 1 - \sum_{e_2=0}^{\infty} \sum_{e_1=0}^{\infty} \Theta_{e_2} \Gamma(\mu_a + e_1, \mathcal{A}_2 \theta) \right. \right. \\ & \left. \left. \times \Gamma(G_Q \mu_b + e_2, \mathcal{B}_2 \theta) \right]^P \right]^{Q-1}. \end{aligned} \quad (29)$$

Utilizing the identity of [eq. 1.111, 47], Eq. (29) can be simplified as

$$\begin{aligned} f_{\theta_{\min}}(\theta) = PQ & \sum_{e_8=0}^{Q-1} \sum_{e_9=0}^{P+Pe_8-1} \Theta_{e_9} \left[ \sum_{s_3=0}^{\infty} \sum_{e_5=0}^{\infty} \frac{\Theta_{e_5} \theta^{G_Q \mu_b + e_5 - 1}}{e^{\mathcal{B}_2 \theta}} \times \Gamma(\mu_a + s_3, \mathcal{A}_2 \theta) + \sum_{s_2=0}^{\infty} \sum_{e_4=0}^{\infty} \frac{\Theta_{e_4} \theta^{\mu_a + s_2 - 1}}{e^{\mathcal{A}_2 \theta}} \right. \\ & \left. \times \Gamma(G_Q \mu_b + e_4, \mathcal{B}_2 \theta) \right] \left[ \sum_{e_2=0}^{\infty} \sum_{e_1=0}^{\infty} \Theta_{e_2} \Gamma(\mu_a + e_1, \mathcal{A}_2 \theta) \times \Gamma(G_Q \mu_b + e_2, \mathcal{B}_2 \theta) \right]^{e_9}, \end{aligned} \quad (30)$$

where  $\Theta_{e_9} = \frac{(Q-1)(P+Pe_8-1)}{(-1)^{-e_8-e_9}}$ . Applying the identity of [eq. 8.352.7, 47], Eq. (30) is further simplified as

$$\begin{aligned} f_{\theta_{\min}}(\theta) = PQ & \sum_{e_8=0}^{Q-1} \sum_{e_9=0}^{P+Pe_8-1} \Theta_{e_9} e^{-(\mathcal{A}_2 + \mathcal{B}_2)\theta} [\gamma_1(\theta)]^{e_9} \times \left[ \sum_{s_3=0}^{\infty} \sum_{e_5=0}^{\infty} \sum_{e_{11}=0}^{\mu_a + s_3 - 1} \Theta_{e_{11}} \theta^{G_Q \mu_b + e_5 + e_{11} - 1} \right. \\ & \left. + \sum_{s_2=0}^{\infty} \sum_{e_4=0}^{\infty} \sum_{e_{10}=0}^{G_Q \mu_b + e_4 - 1} \Theta_{e_{10}} \theta^{\mu_a + s_2 + e_{10} - 1} \right], \end{aligned} \quad (31)$$

where  $\Theta_{e_{10}} = \frac{\Theta_{e_4} \Gamma(e_4 + G_Q \mu_b)}{e_{10}! \mathcal{B}_2^{-e_{10}}}$  and  $\Theta_{e_{11}} = \frac{\Theta_{e_5} \Gamma(e_5 + \mu_a)}{e_{11}! \mathcal{A}_2^{-e_{11}}}$ . Here  $\gamma_1(\theta)$  is denoted as

$$\gamma_1(\theta) = \sum_{e_1=0}^{\infty} \sum_{e_2=0}^{\infty} \sum_{e_{12}=0}^{\mu_a + e_1 - 1} \sum_{e_{13}=0}^{G_Q \mu_b + e_2 - 1} \Theta_{e_{13}} \theta^{(e_{12} + e_{13})} \times e^{-(\mathcal{A}_2 + \mathcal{B}_2)\theta}, \quad (32)$$

where  $\Theta_{e_{13}} = \frac{\mathcal{A}_1 \mathcal{B}_1 \Gamma(e_1 + \mu_a) \mathcal{B}_2^{-G_Q \mu_b - e_2 + e_{13}} \Gamma(e_2 + G_Q \mu_b)}{e_{12}! e_{13}! \mathcal{A}_2^{\mu_a + e_1 - e_{12}}}$ . Applying the multinomial theorem of [eq. 7, 49], we obtain

$$[\gamma_1(\theta)]^{e_9} = \sum_{\omega_{e_9}} (g_{0,0,0,0,\dots}, g_{e_1,e_2,e_{12},e_{13}}, \dots, e_{\infty,\infty,\mu_a+e_1-1,G_Q \mu_b+e_2-1}^{e_9}) \times \Omega_{\omega_{e_9}} e^{-\Lambda_{\omega_{e_9}} \theta} \theta^{\Psi_{\omega_{e_9}}}, \quad (33)$$

where  $(i_1, i_2, \dots, i_m)^i = \frac{i!}{i_1! i_2! \dots i_m!}$  symbolizes the multinomial coefficients,  $\Omega_{\omega_{e_9}} = \prod_{e_1, e_2, e_{12}, e_{13}} \Theta_{e_{13}}^{g_{e_1, e_2, e_{12}, e_{13}}}$ ,  $\Psi_{\omega_{e_9}} = \sum_{e_1} \sum_{e_2} \sum_{e_{12}} \sum_{e_{13}} (e_{12} + e_{13}) g_{e_1, e_2, e_{12}, e_{13}}$  and  $\Lambda_{\omega_{e_9}} = \sum_{e_1} \sum_{e_2} \sum_{e_{12}} \sum_{e_{13}} (\mathcal{A}_2 + \mathcal{B}_2) g_{e_1, e_2, e_{12}, e_{13}}$ . For each element of  $\omega_{e_9}$ , the



sum in Eq. (33) is to be performed, which can be defined as

$$\omega_{e_9} = [(g_{0,0,0,0,\dots}, g_{e_1,e_2,e_{12},e_{13}}, \dots, e_{\infty,\infty,\mu_a+e_1-1,G_Q\mu_b+e_2-1}) : g_{e_1,e_2,e_{12},e_{13}} \in \mathbb{N}, 0 \leq e_1 \leq \infty, 0 \leq e_2 \leq \infty, 0 \leq e_{12} \leq \mu_a + e_1 - 1, 0 \leq e_{13} \leq G_Q\mu_b + e_2 - 1; \sum_{e_1,e_2,e_{12},e_{13}} g_{e_1,e_2,e_{12},e_{13}} = e_9]. \quad (34)$$

Finally, substituting Eq. (33) into Eq. (31), we get

$$f_{\theta_{\min}}(\theta) = \sum_{e_8=0}^{Q-1} \sum_{e_9=0}^{P+P_{e_8}-1} \sum_{\omega_{e_9}} \left( \sum_{s_2=0}^{\infty} \sum_{e_4=0}^{\infty} \sum_{e_{10}=0}^{G_Q\mu_b+e_4-1} \mathcal{J}_1 \theta^{\mathcal{J}_3} + \sum_{s_3=0}^{\infty} \sum_{e_5=0}^{\infty} \sum_{e_{11}=0}^{\mu_a+s_3-1} \mathcal{J}_2 \theta^{\mathcal{J}_4} \right) e^{-\mathcal{J}_5 \theta}, \quad (35)$$

where  $\Theta_{\omega_{e_9}} = (g_{0,0,0,0,\dots}, g_{e_1,e_2,e_{12},e_{13}}, \dots, e_{\infty,\infty,\mu_a+e_1-1,G_Q\mu_b+e_2-1}) \times \Omega_{\omega_{e_9}}$ ,  $\mathcal{J}_1 = PQ\Theta_{e_9}\Theta_{e_{10}}\Theta_{\omega_{e_9}}$ ,  $\mathcal{J}_2 = PQ\Theta_{e_9}\Theta_{e_{11}}\Theta_{\omega_{e_9}}$ ,  $\mathcal{J}_3 = \mu_a + \Psi_{\omega_{e_9}} + s_2 + e_{10} - 1$ ,  $\mathcal{J}_4 = G_Q\mu_b + \Psi_{\omega_{e_9}} + e_5 + e_{11} - 1$ , and  $\mathcal{J}_5 = \mathcal{A}_2 + \mathcal{B}_2 + \Lambda_{\omega_{e_9}}$ .

### E. Modeling of Eavesdropper Channels

In order to perform the secrecy analysis assuming the worst possible case (i.e. maximum strength of the eavesdroppers), we herein, consider maximum SNR among  $W$  eavesdroppers as denoted by  $\theta_{\max} = \max_{1 \leq c \leq W} \theta_c^*$ . Similar to the multicast channels,  $\theta_1^*, \theta_2^*, \dots, \theta_W^*$  are independent, and by means of order statistics, the PDF of  $\theta_{\max}$  is defined as [eq. 40, 38]

$$f_{\theta_{\max}}(\theta) = W f_{*,c}(\theta) [F_{*,c}(\theta)]^{W-1}. \quad (36)$$

Hence, substituting Eq. (26) and Eq. (27) into Eq. (36), and after some mathematical manipulation,  $f_{\theta_{\max}}(\theta)$  is obtained as

$$f_{\theta_{\max}}(\theta) = PW \left[ \sum_{s_4=0}^{\infty} \sum_{e_6=0}^{\infty} \frac{\Theta_{e_6} \theta^{\mu_a+s_4-1}}{e^{\mathcal{A}_2 \theta}} \Gamma(G_W\mu_c + e_6, \mathcal{C}_2 \theta) + \sum_{s_5=0}^{\infty} \sum_{e_7=0}^{\infty} \frac{\Theta_{e_7} \theta^{G_W\mu_c+e_7-1}}{e^{\mathcal{C}_2 \theta}} \Gamma(\mu_a + s_5, \mathcal{A}_2 \theta) \right] \times \left[ 1 - \sum_{e_3=0}^{\infty} \sum_{e_1=0}^{\infty} \Theta_{e_3} \Gamma(\mu_a + e_1, \mathcal{A}_2 \theta) \Gamma(G_W\mu_c + e_3, \mathcal{C}_2 \theta) \right]^{PW-1}. \quad (37)$$

Simplifying Eq. (37) similar to Eq. (31), we get

$$f_{\theta_{\max}}(\theta) = PW \sum_{e_{14}=0}^{PW-1} \Theta_{e_{14}} e^{-(\mathcal{A}_2+\mathcal{C}_2)\theta} [\gamma_3(\theta)]^{e_{14}} \left[ \sum_{s_4=0}^{\infty} \sum_{e_6=0}^{\infty} \sum_{e_{15}=0}^{G_W\mu_c+e_6-1} \Theta_{e_{15}} \theta^{\mu_a+s_4+e_{15}-1} + \sum_{s_5=0}^{\infty} \sum_{e_7=0}^{\infty} \sum_{e_{16}=0}^{\mu_a+s_5-1} \Theta_{e_{16}} \theta^{G_W\mu_c+e_7+e_{16}-1} \right], \quad (38)$$

where  $\Theta_{e_{14}} = (-1)^{e_{14}} \binom{PW-1}{e_{14}}$ ,  $\Theta_{e_{15}} = \frac{\Theta_{e_6} \Gamma(e_6+G_W\mu_c)}{e_{15}! \mathcal{C}_2^{-e_{15}}}$  and  $\Theta_{e_{16}} = \frac{\Theta_{e_7} \Gamma(s_5+\mu_a)}{e_{16}! \mathcal{A}_2^{-e_{16}}}$ . Here,

$$\gamma_3(\theta) = \sum_{e_1=0}^{\infty} \sum_{e_3=0}^{\infty} \sum_{e_{17}=0}^{\mu_a+e_1-1} \sum_{e_{18}=0}^{G_W\mu_c+e_3-1} \Theta_{e_{18}} \theta^{e_{17}+e_{18}} e^{-(\mathcal{A}_2+\mathcal{C}_2)\theta}, \quad (39)$$

where  $\Theta_{e_{18}} = \frac{\mathcal{A}_1 \mathcal{C}_1 \Gamma(e_1+\mu_a) \mathcal{C}_2^{-G_W\mu_c-e_3+e_{18}} \Gamma(e_3+G_W\mu_c)}{e_{17}! e_{18}! \mathcal{A}_2^{\mu_a+e_1-e_{17}}}$ . Implementing multinomial theorem, we get

$$[\gamma_3(\theta)]^{e_{14}} = \sum_{\omega_{e_{14}}} \Theta_{\omega_{e_{14}}} e^{-\Lambda_{\omega_{e_{14}}} \theta} \theta^{\Psi_{\omega_{e_{14}}}}, \quad (40)$$

where  $\Theta_{\omega_{e_{14}}} = \sum_{\omega_{e_{14}}} \times \binom{e_{14}}{h_{0,0,0,0}, \dots, h_{e_1, e_3, e_{17}, e_{18}}, \dots, e_{\infty, \infty, \mu_a + s_5 - 1, G_W \mu_c + e_3 - 1}} \Omega_{\omega_{e_{14}}}$ ,  $\Omega_{\omega_{e_{14}}} = \prod_{e_1, e_3, e_{17}, e_{18}} \Theta_{e_{18}}^{h_{e_1, e_3, e_{17}, e_{18}}}$ ,  $\Psi_{\omega_{e_{14}}} = \sum_{e_1} \sum_{e_3} \sum_{e_{17}} \sum_{e_{18}} (e_{17} + e_{18}) h_{e_1, e_3, e_{17}, e_{18}}$ ,  $\Lambda_{\omega_{e_{14}}} = \sum_{e_1} \sum_{e_3} \sum_{e_{17}} \sum_{e_{18}} (\mathcal{A}_2 + \mathcal{C}_2) h_{e_1, e_3, e_{17}, e_{18}}$ . Finally, substituting Eq. (40) into Eq. (38), we obtain

$$f_{\theta_{\max}}(\theta) = \sum_{e_{14}=0}^{PW-1} \sum_{\omega_{e_{14}}} \left( \sum_{s_4=0}^{\infty} \sum_{e_6=0}^{\infty} \sum_{e_{15}=0}^{G_W \mu_c + e_6 - 1} \mathcal{J}_6 \theta^{\mathcal{J}_8} + \sum_{s_5=0}^{\infty} \sum_{e_7=0}^{\infty} \sum_{e_{16}=0}^{\mu_a + s_5 - 1} \mathcal{J}_7 \theta^{\mathcal{J}_9} \right) e^{-\mathcal{J}_{10} \theta}, \quad (41)$$

where  $\mathcal{J}_6 = PW \Theta_{e_{14}} \Theta_{e_{15}} \Theta_{\omega_{e_{14}}}$ ,  $\mathcal{J}_7 = PW \Theta_{e_{14}} \Theta_{e_{16}} \Theta_{\omega_{e_{14}}}$ ,  $\mathcal{J}_8 = \mu_a + \Psi_{\omega_{e_{14}}} + s_4 + e_{15} - 1$ ,  $\mathcal{J}_9 = G_W \mu_c + \Psi_{\omega_{e_{14}}} + e_7 + e_{16} - 1$ , and  $\mathcal{J}_{10} = \mathcal{A}_2 + \mathcal{C}_2 + \Lambda_{\omega_{e_{14}}}$ .

### 3. PERFORMANCE METRICS

In the following parts, we utilize  $f_{\theta_{\min}}(\theta)$  and  $f_{\theta_{\max}}(\theta)$  of Eq. (35) and Eq. (41) to derive closed-form expressions of three performance metrics i.e. PNSMC, SOPM, and ESMC.

#### A. PNSMC Analysis

Denoting secrecy multicast capacity as  $\mathcal{C}_{s,m}$  [eq. 18, 39], the PNSMC can be expressed as [eq. 25, 50], [51]

$$Pr(\mathcal{C}_{s,m} > 0) = \int_0^{\infty} \int_0^{\theta_b^*} f_{\theta_{\min}}(\theta_b^*) f_{\theta_{\max}}(\theta_c^*) d\theta_c^* d\theta_b^*. \quad (42)$$

Substituting Eq. (35) and Eq. (41) into Eq. (42),  $Pr(\mathcal{C}_{s,m} > 0)$  can be written as

$$\begin{aligned} Pr(\mathcal{C}_{s,m} > 0) &= \int_0^{\infty} \int_0^{\theta_b^*} \sum_{e_8=0}^{Q-1} \sum_{e_9=0}^{P+Pe_8-1} \sum_{\omega_{e_9}} \left( \sum_{s_2=0}^{\infty} \sum_{e_4=0}^{\infty} \sum_{e_{10}=0}^{G_Q \mu_b + e_4 - 1} \mathcal{J}_1 \theta_b^{*\mathcal{J}_3} + \sum_{s_3=0}^{\infty} \sum_{e_5=0}^{\infty} \sum_{e_{11}=0}^{\mu_a + s_3 - 1} \mathcal{J}_2 \theta_b^{*\mathcal{J}_4} \right) \\ &\times e^{-\mathcal{J}_5 \theta_b^*} \sum_{e_{14}=0}^{PW-1} \sum_{\omega_{e_{14}}} \left( \sum_{s_4=0}^{\infty} \sum_{e_6=0}^{\infty} \sum_{e_{15}=0}^{G_W \mu_c + e_6 - 1} \mathcal{J}_6 \theta_c^{*\mathcal{J}_8} + \sum_{s_5=0}^{\infty} \sum_{e_7=0}^{\infty} \sum_{e_{16}=0}^{\mu_a + s_5 - 1} \mathcal{J}_7 \theta_c^{*\mathcal{J}_9} \right) e^{-\mathcal{J}_{10} \theta_c^*} d\theta_c^* d\theta_b^*. \end{aligned} \quad (43)$$

Finally, performing integration making use of [(eq. 3.351.1, 3.351.3), 47], the closed form expression for PNSMC is shown as

$$\begin{aligned} Pr(\mathcal{C}_{s,m} > 0) &= \sum_{e_8=0}^{Q-1} \sum_{e_9=0}^{P+Pe_8-1} \sum_{\omega_{e_9}} \sum_{e_{14}=0}^{PW-1} \sum_{\omega_{e_{14}}} \left[ \sum_{s_2=0}^{\infty} \sum_{e_4=0}^{\infty} \sum_{e_{10}=0}^{G_Q \mu_b + e_4 - 1} \left[ \sum_{s_3=0}^{\infty} \sum_{e_5=0}^{\infty} \sum_{e_{11}=0}^{\mu_a + s_3 - 1} \left( \frac{\omega_1 \mathcal{J}_1 \mathcal{J}_3!}{\mathcal{J}_5^{\mathcal{J}_3+1}} - \sum_{c_2=0}^{\mathcal{J}_8} \right. \right. \right. \\ &\times \left. \left. \frac{\omega_2 \mathcal{J}_1 (\mathcal{J}_3 + \mathcal{J}_8)!}{(\mathcal{J}_5 + \mathcal{J}_{10})^{\mathcal{J}_3 + \mathcal{J}_8 + 1}} \right) + \sum_{s_3=0}^{\infty} \sum_{e_5=0}^{\infty} \sum_{e_{11}=0}^{\mu_a + s_3 - 1} \left( \frac{\omega_1 \mathcal{J}_2 \mathcal{J}_4!}{\mathcal{J}_5^{\mathcal{J}_4+1}} - \sum_{c_2=0}^{\mathcal{J}_8} \frac{\omega_2 \mathcal{J}_2 (\mathcal{J}_4 + \mathcal{J}_8)!}{(\mathcal{J}_5 + \mathcal{J}_{10})^{\mathcal{J}_4 + \mathcal{J}_8 + 1}} \right) \right] + \sum_{s_5=0}^{\infty} \sum_{e_7=0}^{\infty} \sum_{e_{16}=0}^{\mu_a + s_5 - 1} \\ &\times \left[ \sum_{s_2=0}^{\infty} \sum_{e_4=0}^{\infty} \sum_{e_{10}=0}^{G_Q \mu_b + e_4 - 1} \left( \frac{\omega_3 \mathcal{J}_1 \mathcal{J}_3!}{\mathcal{J}_5^{\mathcal{J}_3+1}} - \sum_{c_3=0}^{\mathcal{J}_9} \frac{\omega_4 \mathcal{J}_1 (\mathcal{J}_3 + \mathcal{J}_9)!}{(\mathcal{J}_5 + \mathcal{J}_{10})^{\mathcal{J}_3 + \mathcal{J}_9 + 1}} \right) + \sum_{s_3=0}^{\infty} \sum_{e_5=0}^{\infty} \sum_{e_{11}=0}^{\mu_a + s_3 - 1} \left( \frac{\omega_3 \mathcal{J}_2 \mathcal{J}_4!}{\mathcal{J}_5^{\mathcal{J}_4+1}} \right. \right. \\ &\left. \left. - \sum_{c_3=0}^{\mathcal{J}_9} \frac{\omega_4 \mathcal{J}_2 (\mathcal{J}_4 + \mathcal{J}_9)!}{(\mathcal{J}_5 + \mathcal{J}_{10})^{\mathcal{J}_4 + \mathcal{J}_9 + 1}} \right) \right] \Bigg], \end{aligned} \quad (44)$$

where  $\omega_1 = \frac{\mathcal{J}_6 \mathcal{J}_8!}{\mathcal{J}_{10}^{\mathcal{J}_8+1}}$ ,  $\omega_2 = \frac{\mathcal{J}_6 \mathcal{J}_8!}{c_2! \mathcal{J}_{10}^{\mathcal{J}_8 - c_2 + 1}}$ ,  $\omega_3 = \frac{\mathcal{J}_7 \mathcal{J}_9!}{\mathcal{J}_{10}^{\mathcal{J}_9+1}}$  and  $\omega_4 = \frac{\mathcal{J}_7 \mathcal{J}_9!}{c_3! \mathcal{J}_{10}^{\mathcal{J}_9 - c_3 + 1}}$ .

Note that, in Eq. (44), the PNSMC is expressed in terms of all system parameters that significantly affects the secrecy performance of our proposed system model. It is noteworthy that, for a special case with  $(\kappa_b = \kappa_c = \kappa_a = 0, \mu_b = \mu_c = \mu_a = m, \text{ and } m_b = m_c = m_a \rightarrow \infty)$ , our results using Eq. (44) completely matches with the results obtained with Nakagami- $m$  fading channel (considering uncorrelated case) in [29]. Correspondingly, for the special case with  $P = 0, Q = W = 1, \kappa_b = \kappa_c = \kappa_a = K, \mu_b = \mu_c = \mu_a = 1$  and  $m_b = m_c = m_a = m$ , our analysis implementing Eq. (44) is in a good agreement with [eq. 25, 52].

## B. SOPM Analysis

Signifying the target secrecy rate by  $\xi_s$ , the SOPM is denoted as [eq. 20, 53], [54]

$$\begin{aligned} P_{out}(\xi_s) &= Pr(\mathcal{C}_{s,m} < \xi_s) \\ &= 1 - \int_0^\infty \int_{\psi_s}^\infty f_{\theta_{min}}(\theta_b^*) f_{\theta_{max}}(\theta_c^*) d\theta_b^* d\theta_c^*, \end{aligned} \quad (45)$$

where  $\psi_s = 2^{\xi_s}(1 + \theta_c^*) - 1$  and  $\xi_s > 0$ . This definition specifies that, reliable transmission is achievable only if  $\mathcal{C}_{s,m} > \xi_s$ , otherwise the security can not be guaranteed. Substituting Eq. (35) and Eq. (41) into Eq. (45), we get

$$\begin{aligned} P_{out}(\xi_s) &= \int_0^\infty \int_{\psi_s}^\infty \sum_{e_8=0}^{Q-1} \sum_{e_9=0}^{P+Pe_8-1} \sum_{\omega_{e_9}} \left( \sum_{s_2=0}^\infty \sum_{e_4=0}^\infty \sum_{e_{10}=0}^{G_Q\mu_b+e_4-1} \mathcal{J}_1 \theta_b^{*\mathcal{J}_3} + \sum_{s_3=0}^\infty \sum_{e_5=0}^\infty \sum_{e_{11}=0}^{\mu_a+s_3-1} \mathcal{J}_2 \theta_b^{*\mathcal{J}_4} \right) \\ &\quad \times e^{-\mathcal{J}_5 \theta_b^*} \sum_{e_{14}=0}^{PW-1} \sum_{\omega_{e_{14}}} \left( \sum_{s_4=0}^\infty \sum_{e_6=0}^\infty \sum_{e_{15}=0}^{G_W\mu_c+e_6-1} \mathcal{J}_6 \theta_c^{*\mathcal{J}_8} + \sum_{s_5=0}^\infty \sum_{e_7=0}^\infty \sum_{e_{16}=0}^{\mu_a+s_5-1} \mathcal{J}_7 \theta_c^{*\mathcal{J}_9} \right) e^{-\mathcal{J}_{10} \theta_c^*} d\theta_b^* d\theta_c^*. \end{aligned} \quad (46)$$

Now, performing integration making use of [(eq. 3.351.2, 3.351.3), 47] in Eq. (46), the closed form expression for the SOPM is shown as

$$\begin{aligned} P_{out}(\xi_s) &= 1 - \sum_{e_8=0}^{Q-1} \sum_{e_9=0}^{P+Pe_8-1} \sum_{\omega_{e_9}} \sum_{e_{14}=0}^{PW-1} \sum_{\omega_{e_{14}}} \left[ \sum_{s_2=0}^\infty \sum_{e_4=0}^\infty \sum_{e_{10}=0}^{G_Q\mu_b+e_4-1} \sum_{f_2=0}^{\mathcal{J}_3} \sum_{f_4=0}^{\mathcal{J}_2} \left[ \sum_{s_4=0}^\infty \sum_{e_6=0}^\infty \sum_{e_{15}=0}^{G_W\mu_c+e_6-1} \frac{\mathcal{J}_6 \omega_5 (\mathcal{J}_8 + f_4)!}{(\mathcal{J}_{10} + \mathcal{J}_5 q_{\psi_s})^{\mathcal{J}_8+f_4+1}} \right. \right. \\ &\quad + \left. \sum_{s_5=0}^\infty \sum_{e_7=0}^\infty \sum_{e_{16}=0}^{\mu_a+s_5-1} \frac{\mathcal{J}_7 \omega_5 (\mathcal{J}_9 + f_4)!}{(\mathcal{J}_{10} + \mathcal{J}_5 q_{\psi_s})^{\mathcal{J}_9+f_4+1}} \right] - \sum_{s_3=0}^\infty \sum_{e_5=0}^\infty \sum_{e_{11}=0}^{\mu_a+s_3-1} \sum_{f_3=0}^{\mathcal{J}_4} \sum_{f_5=0}^{\mathcal{J}_3} \left[ \sum_{s_4=0}^\infty \sum_{e_6=0}^\infty \sum_{e_{15}=0}^{G_W\mu_c+e_6-1} \right. \\ &\quad \times \left. \frac{\mathcal{J}_6 \omega_6 (\mathcal{J}_8 + f_5)!}{(\mathcal{J}_{10} + \mathcal{J}_5 q_{\psi_s})^{\mathcal{J}_8+f_5+1}} + \sum_{s_5=0}^\infty \sum_{e_7=0}^\infty \sum_{e_{16}=0}^{\mu_a+s_5-1} \frac{\mathcal{J}_7 \omega_6 (\mathcal{J}_9 + f_5)!}{(\mathcal{J}_{10} + \mathcal{J}_5 q_{\psi_s})^{\mathcal{J}_9+f_5+1}} \right] \Bigg], \end{aligned} \quad (47)$$

where  $p_{\psi_s} = 2^{\xi_s} - 1$ ,  $q_{\psi_s} = 2^{\xi_s}$ ,  $\omega_5 = \frac{\mathcal{J}_1 \mathcal{J}_3! (f_2!) p_{\psi_s}^{f_2-f_4}}{f_2! \mathcal{J}_5^{\mathcal{J}_3-f_2+1} q_{\psi_s}^{f_4} e^{\mathcal{J}_5 p_{\psi_s}}}$  and  $\omega_6 = \frac{\mathcal{J}_2 \mathcal{J}_4! (f_3!) p_{\psi_s}^{f_3-f_5}}{f_3! \mathcal{J}_5^{\mathcal{J}_4-f_3+1} q_{\psi_s}^{f_5} e^{\mathcal{J}_5 p_{\psi_s}}}$ .

It can be seen that, Eq. (47) comprises of all the system parameters of the proposed network which helps to evaluate the secrecy outage performance of the proposed system in terms of best relaying. Note that, as a special case of the proposed network with  $\kappa_a = K$ ,  $\mu_a = 1$  and  $m_a = m$ , we obtain Shadowed Rician fading distribution for satellite links and for  $\kappa_b = \kappa_c = 0$ ,  $\mu_b = \mu_c = m$  and  $m_b = m_c \rightarrow \infty$ , we obtain Nakagami- $m$  fading distribution for terrestrial links. For this particular case our results with Eq. (47) totally matches with [eq. 45, 55]. Likewise, for a special case with ( $\kappa_b = \kappa_c = \kappa_a = 0$ ,  $\mu_b = \mu_c = \mu_a = m$ , and  $m_b = m_c = m_a \rightarrow \infty$ ), our results with Eq. (47) can be shown similar to uncorrelated (correlation coefficient  $\rightarrow 0$ ) Nakagami- $m$  fading channel in [29].

## C. ESMC Analysis

The ESMC can be defined as [eq. 4, 56]

$$\langle \mathcal{C}_{s,m} \rangle = \int_0^\infty \log_2(1 + \theta_b^*) f_{\theta_{min}}(\theta_b^*) d\theta_b^* - \int_0^\infty \log_2(1 + \theta_c^*) f_{\theta_{max}}(\theta_c^*) d\theta_c^*. \quad (48)$$

Replacing Eq. (35) and Eq. (41) into Eq. (48) and integrating by making use of [eq. 4.222.8, 47], the novel expression for the ESMC is exhibited as

$$\begin{aligned}
\langle C_{s,m} \rangle = & \sum_{e_8=0}^{Q-1} \sum_{e_9=0}^{P+Pe_8-1} \sum_{\omega_{e_9}} \left[ \sum_{s_2=0}^{\infty} \sum_{e_4=0}^{\infty} \sum_{e_{10}=0}^{G_Q \mu_b + e_4 - 1} \left[ \sum_{d_2=0}^{\mathcal{J}_3} \frac{D_5}{\ln(2)} \frac{(-1)^{D_1-1} Ei(-\mathcal{J}_5)}{(\frac{1}{\mathcal{J}_5})^{D_1} e^{-\mathcal{J}_5}} + \sum_{d_3=1}^{D_1} \frac{(d_3-1)!}{(-\frac{1}{\mathcal{J}_5})^{D_1-d_3}} \right] + \sum_{s_3=0}^{\infty} \sum_{e_5=0}^{\infty} \right. \\
& \times \sum_{e_{11}=0}^{\mu_a + s_3 - 1} \left[ \sum_{d_4=0}^{\mathcal{J}_4} \frac{D_6}{\ln(2)} \frac{(-1)^{D_2-1} Ei(-\mathcal{J}_5)}{(\frac{1}{\mathcal{J}_5})^{D_2} e^{-\mathcal{J}_5}} + \sum_{d_5=1}^{D_2} \frac{(d_5-1)!}{(-\frac{1}{\mathcal{J}_5})^{D_2-d_5}} \right] - \sum_{e_{14}=0}^{PW-1} \sum_{\omega_{e_{14}}} \left[ \sum_{s_4=0}^{\infty} \sum_{e_6=0}^{\infty} \sum_{e_{15}=0}^{G_W \mu_c + e_6 - 1} \right. \\
& \times \left[ \sum_{d_6=0}^{\mathcal{J}_8} \frac{D_7}{\ln(2)} \frac{(-1)^{D_3-1} Ei(-\mathcal{J}_{10})}{(\frac{1}{\mathcal{J}_{10}})^{D_3} e^{-\mathcal{J}_{10}}} + \sum_{d_7=1}^{D_3} \frac{(d_7-1)!}{(-\frac{1}{\mathcal{J}_{10}})^{D_3-d_7}} \right] - \sum_{s_5=0}^{\infty} \sum_{e_7=0}^{\infty} \sum_{e_{16}=0}^{\mu_a + s_5 - 1} \left[ \sum_{d_8=0}^{\mathcal{J}_9} \frac{D_8}{\ln(2)} \frac{(-1)^{D_4-1} Ei(-\mathcal{J}_{10})}{(\frac{1}{\mathcal{J}_{10}})^{D_4} e^{-\mathcal{J}_{10}}} \right. \\
& \left. \left. + \sum_{d_9=1}^{D_4} \frac{(d_9-1)!}{(-\frac{1}{\mathcal{J}_{10}})^{D_4-d_9}} \right] \right], \tag{49}
\end{aligned}$$

where  $D_1 = \mathcal{J}_3 - d_2$ ,  $D_2 = \mathcal{J}_4 - d_4$ ,  $D_3 = \mathcal{J}_8 - d_6$ ,  $D_4 = \mathcal{J}_9 - d_8$ ,  $D_5 = \frac{\mathcal{J}_1 \mathcal{J}_3!}{D_1! \mathcal{J}_5^{\mathcal{J}_3+1}}$ ,  $D_6 = \frac{\mathcal{J}_2 \mathcal{J}_4!}{D_2! \mathcal{J}_5^{\mathcal{J}_4+1}}$ ,  $D_7 = \frac{\mathcal{J}_6 \mathcal{J}_8!}{D_3! \mathcal{J}_{10}^{\mathcal{J}_8+1}}$ , and  $D_8 = \frac{\mathcal{J}_7 \mathcal{J}_9!}{D_4! \mathcal{J}_{10}^{\mathcal{J}_9+1}}$ .

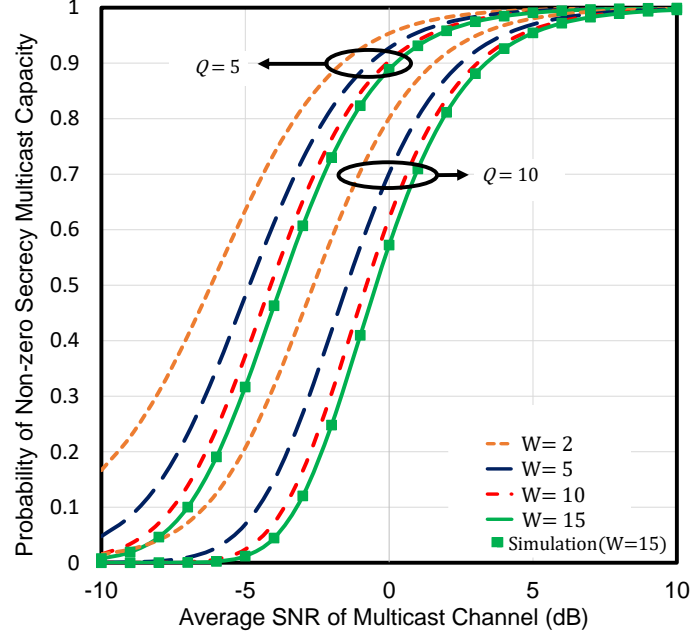
It is clear that how do the physical properties of the channels as well as the system parameters affects the secrecy capacity, can be easily quantified with Eq. (49). It is noted that, as a special case of Shadowed Rician fading distribution with ( $P = 0$ ,  $Q = W = 1$   $\kappa_b = \kappa_c = \kappa_a = K$ ,  $\mu_b = \mu_c = \mu_a = 1$  and  $m_b = m_c = m_a \rightarrow m$ ), our obtained results with Eq. (49) are equivalent with the analysis in [eq. 51, 52]. In parallel, utilizing Eq. (49), another special scenario i.e. Shadowed Rician fading distribution for satellite links and Rayleigh fading distribution ( $Q = W = 1$ ,  $\kappa_b = \kappa_c = \kappa_a = 0$ ,  $\mu_b = \mu_c = \mu_a = 1$  and  $m_b = m_c = m_a \rightarrow \infty$ ) for terrestrial links can be shown as a special case of our model [57].

#### 4. NUMERICAL RESULTS

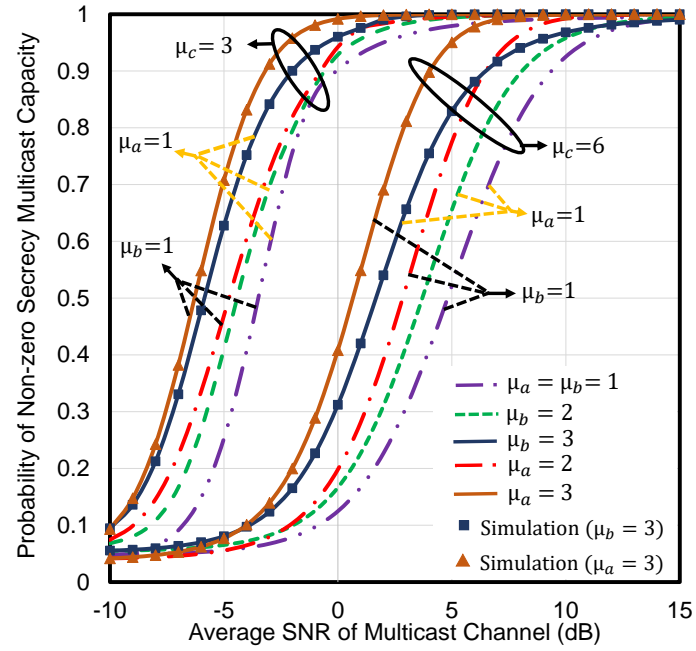
In this section, the numerical results concerning the expressions of PNSMC, SOPM, and ESMC as given in Eq. (44), Eq. (47), and Eq. (49), respectively are demonstrated graphically in order to gain some useful insights regarding the enhancement of security by taking the advantages of the physical properties of the propagation medium. Since the infinite series converges rapidly after a few terms, we take the first 100 terms to obtain the numerical results. Additionally, we also carry out the Monte-Carlo (MC) simulations to authenticate the mathematical expressions. To accomplish this task, we generate  $\kappa - \mu$  shadowed random variables in MATLAB and average  $10^6$  random samples.

Figure 2 presents the PNSMC against  $\bar{\theta}_{ab}$  in which the impact of the multicast receivers ( $Q$ ) and eavesdroppers ( $W$ ) are illustrated. We assume two scenarios considering  $Q = 5$  and 10. Both the scenarios clearly dictate that the PNSMC decreases with increasing values of  $Q$ , and  $W$ . In the multicast scenario, due to the increase in  $Q$ , the bandwidth per user is reduced which causes a reduction in the received SNR at the user node. Hence the PNSMC performance degrades remarkably which is testified in [29]. On the contrary, increasing  $W$  escalates the strength of the eavesdroppers by ensuring the maximum SNR at the eavesdropper node (since increasing  $W$  indicates an increasing probability of obtaining maximum SNR at the eavesdropper channel) and thus PNSMC is degraded. This similar outcome is achieved in [58], which justifies our analytical results. It is also observed from Fig. 2 that the MC and analytical simulation are in a good agreement, which clearly indicates the exactness of our PNSMC expression in Eq. (44).

In Fig. 3, the PNSMC is plotted against  $\bar{\theta}_{ab}$  in which the effect of different number of clusters of relay channel ( $\mu_a$ ), multicast channels ( $\mu_b$ ) as well as eavesdropper channel ( $\mu_c$ ) are shown. It is observed from the figure that the increment in the number of clusters of relay ( $\mu_a$ ) and multicast channels ( $\mu_b$ ) enhances the PNSMC of the proposed model. Because, with increasing values of  $\mu_a$  and  $\mu_b$ , we are increasing the end-to-end SNR indirectly by including more incoming signals based on various diversity schemes. As a result, the total fading of the multicast channels reduces which ensures the increment of the PNSMC. Due to this similar reason, the PNSMC of the system degrades with  $\mu_c$ . It is noteworthy that the impact of  $\mu_a$  upgrading the secrecy performance



**Fig. 2.** The PNSMC versus  $\bar{\theta}_{ab}$  for selected values of  $Q$  and  $W$  when  $\bar{\theta}_{ac} = -10dB, G_Q = G_W = 2, \mu_a = \mu_b = \mu_c = 2, \kappa_a = \kappa_b = \kappa_c = 2$ , and  $m_a = m_b = m_c = \infty$ .



**Fig. 3.** The PNSMC versus  $\bar{\theta}_{ab}$  for selected values of  $\mu_b, \mu_a$ , and  $\mu_c$  when  $m_a = m_b = m_c = \infty, \kappa_a = \kappa_b = \kappa_c = 1$ , and  $\bar{\theta}_{ac} = 0dB$ .

is much superior than that of  $\mu_b$ . The outcomes from [27] and [59] exhibits the same characteristics which validate our result convincingly.

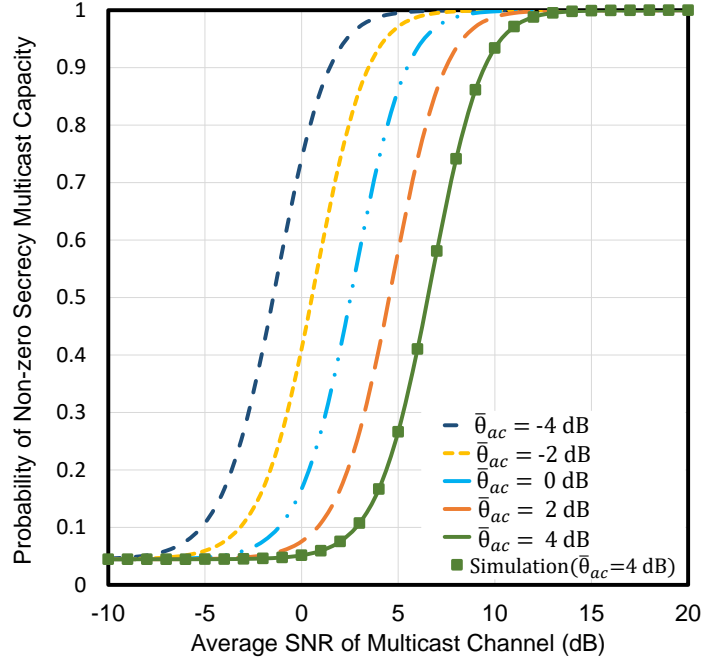


**Fig. 4.** The PNSMC versus  $\bar{\theta}_{ab}$  for selected values of  $\bar{\theta}_{ac}$  when  $G_Q = G_W = 2$ ,  $\mu_a = \mu_b = \mu_c = 2$ ,  $\kappa_a = \kappa_b = \kappa_c = 1$ , and  $m_a = m_b = m_c = \infty$ .

The MC simulation and analytical results of PNSMC as a function of  $\bar{\theta}_{ab}$  is shown in Fig. 4, where the outcomes due to the variation in average SNR of the eavesdropper channel ( $\bar{\theta}_{ac}$ ) are depicted. It is noted that the PNSMC is degraded with the increase of  $\bar{\theta}_{ac}$  because an increase in  $\bar{\theta}_{ac}$  indicates a higher SNR at the eavesdropper terminals which enhances the strength of the wiretap channels in terms of secrecy performance as shown in [60, 61].

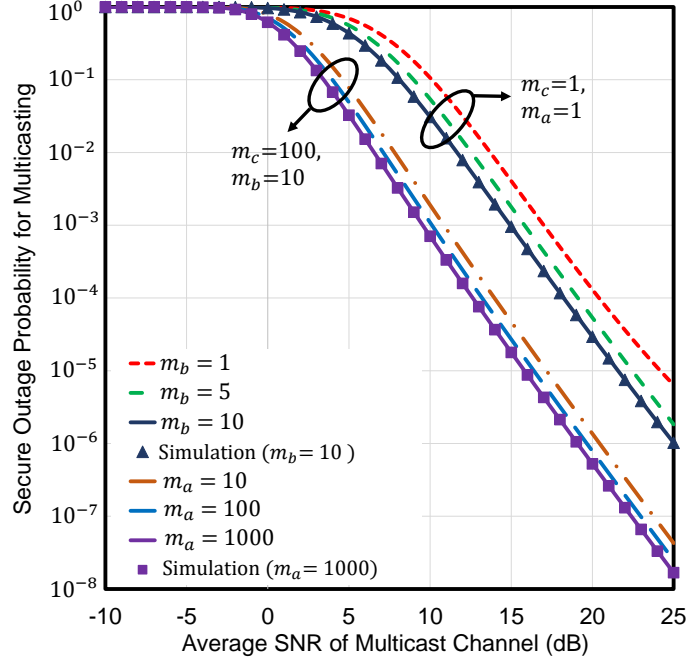
Figure 5 demonstrates the SOPM as a function of  $\bar{\theta}_{ab}$ , where the consequences of variation in the shadowing parameter for multicast channels ( $m_b$ ) and relay channel ( $m_a$ ) are represented. From the figure, it is recognized that increment in  $m_b$  and  $m_a$  minimize the shadowing effect of the multicast channel, and thus the SOPM of the model decrease. So superior secrecy performance can be achieved if the shadowing present in the multicast network is comparatively lower. Our numerical result is also confirmed by MC simulation. A similar conclusion (related to shadowing) was also drawn in [27].

Figure 6 depicts SOPM versus  $\bar{\theta}_{ab}$  to represent the effect of target secrecy rate ( $\zeta_s$ ) on the secure outage performance. We consider two cases herein with  $\bar{\theta}_{ac} = 0$  and  $-10$  dB. It is noted that the SOPM increases with  $\zeta_s$  for both cases of  $\bar{\theta}_{ac}$  as shown in [58, 62]. It is also noticeable that the impact of  $\zeta_s$  in case of  $\bar{\theta}_{ac} = -10$  dB is more significant than that of  $\bar{\theta}_{ac} = 0$  dB. Moreover, the SOPM performance improves when the eavesdropper channel becomes worse (i.e.  $\bar{\theta}_{ac} = -10$  dB). A good agreement between MC and analytical outcomes proves that the SOPM derived in Eq. (47) is accurate.

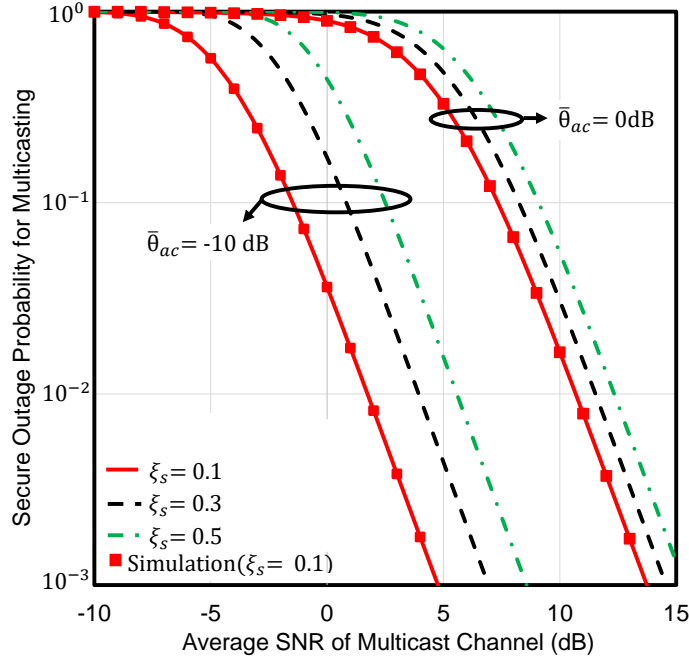
In Fig. 7, the SOPM is varied against  $\bar{\theta}_{ab}$  to illustrate the consequences of differing the number of relays ( $P$ ). From the figure, it can be seen that an increment in  $P$  offers a remarkable improvements in system's SOPM performance. As the number of relays are increased, the  $P$  relays compete among themselves to be the best one. Additionally, the cooperative diversity provided by multiple relays also play a notable role in reducing the impacts of fading and shadowing of multicast links. Similar conclusions were made in [38] that matches our results.

Figure. 8 represents ESMC with respect to  $\bar{\theta}_{ab}$  for different values of  $\kappa_a$ ,  $\kappa_b$  and  $\kappa_c$ . It is evident from the





**Fig. 5.** The SOPM versus  $\bar{\theta}_{ab}$  for selected values of  $m_b$ ,  $m_a$ , and  $m_c$  when  $\bar{\theta}_{ac} = -5\text{dB}$ ,  $G_Q = G_W = 2$ ,  $\mu_a = \mu_b = \mu_c = 1$ , and  $\kappa_a = \kappa_b = \kappa_c = 1$ .



**Fig. 6.** The SOPM versus  $\bar{\theta}_{ab}$  for selected values of  $\xi_s$  and  $\bar{\theta}_{ac}$ .

figure that both  $\kappa_a$  and  $\kappa_b$  increases the secrecy capacity of the proposed system. The increment of  $\kappa_a$  and  $\kappa_b$  enhances the dominant component as well as reduces the scattering component of the multicast channel which

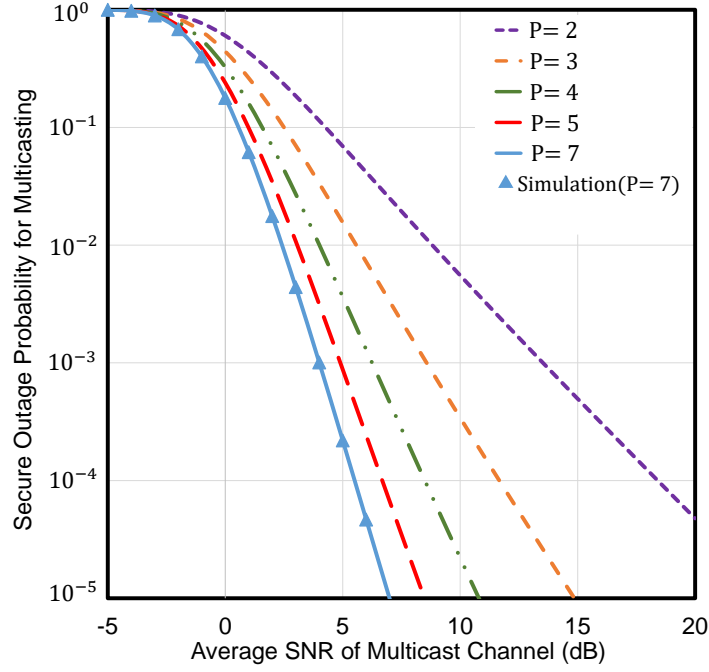


**Fig. 7.** The SOPM versus  $\bar{\theta}_{ab}$  for selected values of  $P$  when  $\bar{\theta}_{ac} = -10\text{dB}$ ,  $G_Q = G_W = 2$ ,  $\mu_a = \mu_b = \mu_c = 1$ ,  $\kappa_a = \kappa_b = \kappa_c = 1$ , and  $m_a = m_b = m_c = \infty$ .

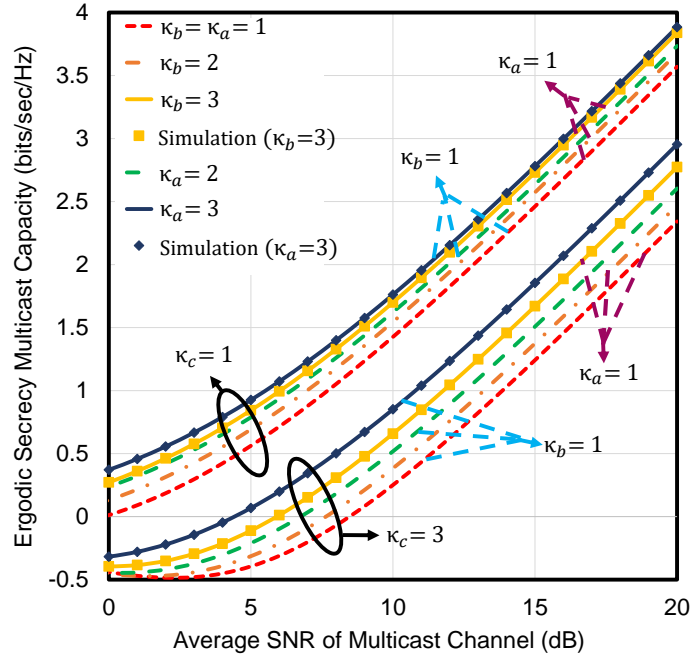


**Fig. 8.** The ESMC versus  $\bar{\theta}_{ab}$  for selected values of  $\kappa_b$ ,  $\kappa_a$ , and  $\kappa_c$  when  $\mu_a = \mu_b = \mu_c = 1$ ,  $m_a = m_b = m_c = \infty$  and  $\bar{\theta}_{ac} = -5\text{dB}$ .

results in higher SNR at the receiver and ESMC of the proposed model. But, the capacity degrades sharply with  $\kappa_c$  as it upgrades the SNR of the eavesdropper channel. Same results were obtained in [27], and [59] which undoubtedly confirms our analysis. The MC simulation also has a tight agreement with the analytical result.

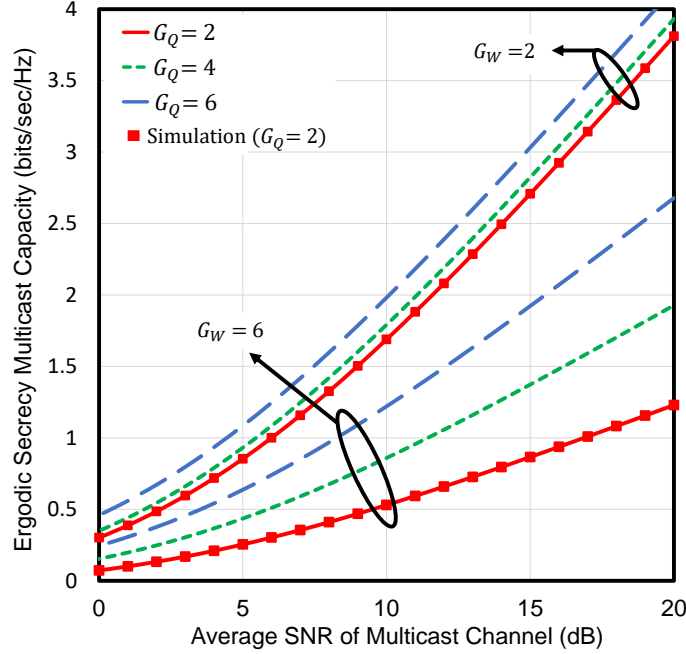


**Fig. 9.** The ESMC versus  $\bar{\theta}_{ab}$  for selected values of  $G_Q$  and  $G_W$  when  $\bar{\theta}_{ac} = -10\text{dB}$ ,  $\kappa_a = \kappa_b = \kappa_c = 1$ ,  $\mu_a = \mu_b = \mu_c = 1$ , and  $m_a = m_b = m_c = \infty$ .

In Fig. 9, ESMC is plotted against  $\bar{\theta}_{ab}$  with a view to observing the impacts due to the variation in number of antennas of each user ( $G_Q$ ) and eavesdropper ( $G_W$ ). From the figure, it is observed that the ESMC escalates if  $G_Q$  increases. This is because an increase in  $G_Q$  significantly reduce the fading of multicast channels by enhancing the antenna diversity at the receiver. On the other hand, it is also noted that, ESMC degrades if  $G_W$  is increased. In that case, the eavesdroppers are capable of overhearing more confidential messages from the multicast channels due to increase in antenna diversity at the eavesdropper terminals. Even ESMC degrades dramatically when the eavesdroppers are equipped with large number of antennas (i.e.  $G_W=6$ ). Similar outcomes are also presented in [41] which manifest the exactness of our results.

### Comparison with Existing Related Literature:

We consider generalized distribution (i.e.  $\kappa - \mu$  shadowed fading) at  $S \rightarrow P$ ,  $P \rightarrow Q$ , and  $P \rightarrow W$  links in the proposed dual-hop scheme that encompasses a number of well-known fading distributions which can be acquired as special cases of our model as shown in Table 1. Hence, it is noteworthy that the derived expressions in Eq. (44), Eq. (47), and Eq. (49) regarding our proposed scenario are also generalized, and can be utilized to unify the secrecy performances of the mentioned channels in Table 1.

Figure 10 exhibits a graphical representation in which the generic characteristics of the proposed scenario is illustrated by plotting ESMC against  $\bar{\theta}_{ab}$ . Note that the secrecy analysis over generalized shadowed model using opportunistic relaying is absent in the previous studies. Moreover, simply reorienting the system parameters, we can generate some existing models as special cases which is a clear indication of superiority of our proposed work. Hence, the conclusive remarks based on the aforementioned discussion is that this novel proposed work is more purposeful than all the conventional multipath/ shadowed secure models.

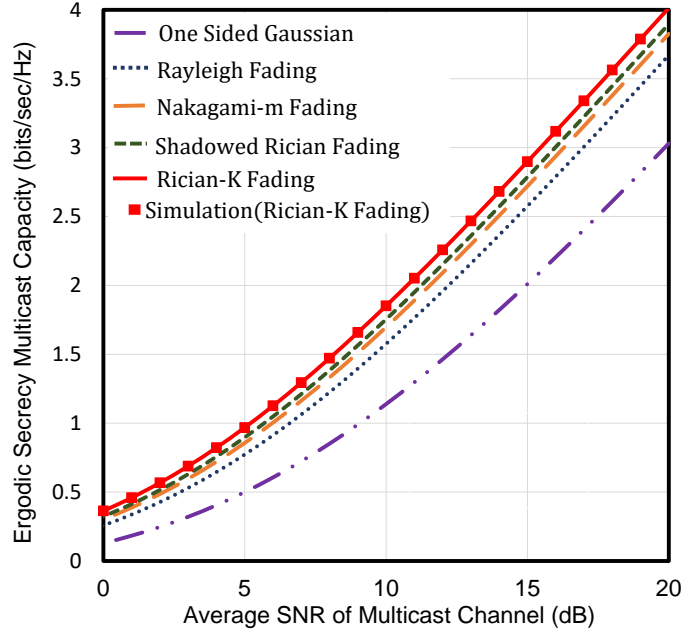


**Fig. 10.** The ESMC versus  $\bar{\theta}_{ab}$  for comparing performance of different classical fading channels as a special cases of  $\kappa - \mu$  shadowed fading channel when  $\bar{\theta}_{ac} = -10\text{dB}$ ,  $G_Q = G_W = 2$ , and  $P = Q = W = 2$ .

## 5. CONCLUSION

This paper deals with the dual-hop secure wireless multicast relaying networks over  $\kappa - \mu$  shadowed fading channels in the presence of multiple eavesdroppers. Enhancement in security is ensured by choosing the best relay among several relays. The effect of all the system parameters on the secrecy performance of the proposed model is thoroughly observed by deriving the exact and closed-form expressions of the performance metrics i.e. PNSMC, SOPM, and ESMC, and then presenting some numerical results based on those expressions which are further authenticated via Monte-Carlo simulations. This analysis has brought out some interesting facts about the proposed system such as the secrecy performance of this dual-hop RF-RF communication model mostly affected by the channel environment of the first hop (i.e.  $\mu_a, \kappa_a$ , etc. of  $S \rightarrow P$  link) than that of the second hops ( $P \rightarrow Q$  and  $P \rightarrow W$  links). Shadowing is an important aspect of this work and the security of this proposed scenario can be increased by increasing the shadowing at  $P \rightarrow W$  link. The proposed generalized shadowed model with opportunistic relaying can also be employed to improve the security of different classical fading scenarios irrespective of the harsh channel conditions in the presence of a large number of multicast receivers and eavesdroppers. The proposed model also exhibits uniqueness since it can be applied in satellite communication where shadowing is one of the major constraints against secure multicast communication.

## REFERENCES

1. N. Simmons, C. R. N. da Silva, S. L. Cotton, P. C. Sofotasios, and M. D. Yacoub, "Double shadowing the Rician fading model," *IEEE Wirel. Commun. Lett.* **8**, 344–347 (2018).
2. N. Y. Ermolova and O. Tirkkonen, "Outage probability over composite  $\eta$ - $\mu$  fading-shadowing radio channels," *IET communications* **6**, 1898–1902 (2012).
3. J. Zhang, L. Dai, W. H. Gerstacker, and Z. Wang, "Effective capacity of communication systems over  $\kappa$ - $\mu$  shadowed fading channels," *Electron. Lett.* **51**, 1540–1542 (2015).
4. C. García-Corrales, F. J. Cañete, and J. F. Paris, "Capacity of  $\kappa$ - $\mu$  shadowed fading channels," *Int. J. Antennas Propag.* **2014** (2014).
5. F. J. Lopez-Martinez, J. F. Paris, and J. M. Romero-Jerez, "The  $\kappa$ - $\mu$  shadowed fading model with integer fading parameters," *IEEE Transactions on Veh. Technol.* **66**, 7653–7662 (2017).
6. S. K. Yoo, N. Bhargava, S. L. Cotton, P. C. Sofotasios, M. Matthaiou, M. Valkama, and G. K. Karagiannidis, "The  $\kappa$ - $\mu$ /inverse gamma and  $\eta$ - $\mu$ /inverse gamma composite fading models: Fundamental statistics and empirical validation," *IEEE Trans. Commun.* p. 1 (2017).
7. D. Pant, P. S. Chauhan, S. K. Soni, and S. Naithani, "Channel capacity analysis of wireless system under ORA scheme over  $\kappa - \mu$  /- inverse gamma

- and  $\eta - \mu$  /-inverse gamma composite fading models," in *2020 International Conference on Electrical and Electronics Engineering (ICE3)*, (IEEE, 2020), pp. 425–430.
8. D. Pant, P. S. Chauhan, and S. K. Soni, "Error probability and channel capacity analysis of wireless system over inverse gamma shadowed fading channel with selection diversity," *Int. J. Commun. Syst.* **32**, e4083 (2019).
  9. P. Raghunwanshi and K. Kumar, " $\alpha - \eta - \mu$ /IG composite fading model for body-centric communication," in *Advances in VLSI, Communication, and Signal Processing*, (Springer, 2021), pp. 263–269.
  10. S. L. Cotton, "Human body shadowing in cellular device-to-device communications: Channel modeling using the shadowed  $\kappa$ - $\mu$  fading model," *IEEE J. on Sel. Areas Commun.* **33**, 111–119 (2014).
  11. Y. J. Chun, S. L. Cotton, H. S. Dhillon, F. J. Lopez-Martinez, J. F. Paris, and S. K. Yoo, "A comprehensive analysis of 5G heterogeneous cellular systems operating over  $\kappa$ - $\mu$  shadowed fading channels," *IEEE Transactions on Wirel. Commun.* **16**, 6995–7010 (2017).
  12. H. Al-Hmood and H. Al-Raweshidy, "Analysis of energy detection with diversity receivers over non-identically distributed  $\kappa$ - $\mu$  shadowed fading channels," *Electron. Lett.* **53**, 83–85 (2016).
  13. J. F. Paris, "Statistical characterization of  $\kappa$ - $\mu$  shadowed fading," *IEEE Transactions on Veh. Technol.* **63**, 518–526 (2013).
  14. S. Parthasarathy and R. K. Ganti, "Coverage analysis in downlink poisson cellular network with  $\kappa$ - $\mu$  shadowed fading," *IEEE Wirel. Commun. Lett.* **6**, 10–13 (2016).
  15. M. R. Bhatnagar, "On the sum of correlated squared  $\kappa$ - $\mu$  shadowed random variables and its application to performance analysis of MRC," *IEEE Transactions on Veh. Technol.* **64**, 2678–2684 (2014).
  16. X. Li, J. Li, L. Li, J. Jin, J. Zhang, and D. Zhang, "Effective rate of MISO systems over  $\kappa$ - $\mu$  shadowed fading channels," *IEEE Access* **5**, 10605–10611 (2017).
  17. J. Zhang, X. Chen, K. P. Peppas, X. Li, and Y. Liu, "On high-order capacity statistics of spectrum aggregation systems over  $\kappa$ - $\mu$  and  $\kappa$ - $\mu$  shadowed fading channels," *IEEE Transactions on Commun.* **65**, 935–944 (2016).
  18. S. K. Yoo, S. L. Cotton, P. C. Sofotasios, and S. Freear, "Shadowed fading in indoor off-body communication channels: A statistical characterization using the  $\kappa$ - $\mu$  / Gamma composite fading model," *IEEE Transactions on Wirel. Commun.* **15**, 5231–5244 (2016).
  19. A. Subhash, M. Srinivasan, and S. Kalyani, "Asymptotic maximum order statistic for SIR in  $\kappa$ - $\mu$  shadowed fading," *IEEE Transactions on Commun.* **67**, 6512–6526 (2019).
  20. L. Han and J. Mu, "Outage probability of opportunistic decode-and-forward relaying over correlated shadowed fading channels," *Wirel. Pers. Commun.* **91**, 453–462 (2016).
  21. J. Zhang and G. Pan, "Secrecy outage analysis with  $k$ th best relay selection in dual-hop inter-vehicle communication systems," *AEU-International J. Electron. Commun.* **71**, 139–144 (2017).
  22. J. Vegasanchez, D. P. M. Osorio, F. J. Lopez-Martinez, M. C. P. Paredes, and L. Urquiza-Aguilar, "Information-theoretic security of mimo networks under-shadowed fading channels," *IEEE Transactions on Veh. Technol.* (2021).
  23. A. S. Sumona, M. K. Kundu, and A. Badrudduza, "Security analysis in multicasting over shadowed rician and  $\alpha - \mu$  fading channels: A dual-hop hybrid satellite terrestrial relaying network," *arXiv preprint arXiv:2105.12071* (2021).
  24. S. Jiang-Feng, L. Xing-Wang, D. Yuan, and D. Jian-He, "Physical layer security over SIMO  $\kappa$ - $\mu$  shadowed fading channels," *Recent Adv. Electr. & Electron. Eng. (Formerly Recent Patents on Electr. & Electron. Eng.* **13**, 871–878 (2020).
  25. M. Nunes and U. S. Dias, "On the physical layer security under  $\kappa$ - $\mu$  shadowed fading channels with diversity approaches," in *Proc. Symp. Telecommun. Processing of Sig.(BSTPS), Brazil*, (2017), pp. 373–377.
  26. Y. Ai, L. Kong, and M. Cheffena, "Secrecy outage analysis of double shadowed Rician channels," *Electron. Lett.* **55**, 765–767 (2019).
  27. J. Sun, H. Bie, X. Li, J. Zhang, G. Pan, and K. M. Rabie, "Secrecy performance analysis of SIMO systems over correlated  $\kappa$ - $\mu$  shadowed fading channels," *IEEE Access* **7**, 86090–86101 (2019).
  28. J. Sun, X. Li, M. Huang, Y. Ding, J. Jin, and G. Pan, "Performance analysis of physical layer security over  $\kappa$ - $\mu$  shadowed fading channels," *IET communications* **12**, 970–975 (2018).
  29. A. Badrudduza, M. Sarkar, and M. K. Kundu, "Enhancing security in multicasting through correlated Nakagami-m fading channels with opportunistic relaying," *Phys. Commun.* **43**, 101177 (2020).
  30. H. Yu and G. L. Stuber, "General decode-and-forward cooperative relaying with co-channel interference in shadowed Nakagami fading channels," *IEEE transactions on wireless communications* **11**, 4318–4327 (2012).
  31. Y. Feng, V. C. Leung, and F. Ji, "Performance study for SWIPT cooperative communication systems in shadowed Nakagami fading channels," *IEEE Transactions on Wirel. Commun.* **17**, 1199–1211 (2017).
  32. A. Iqbal and K. M. Ahmed, "Integrated satellite-terrestrial system capacity over mix shadowed Rician and Nakagami channels," *Int. J. Commun. Networks Inf. Secur.* **5**, 104–109 (2013).
  33. L. Fan, R. Zhao, F.-K. Gong, N. Yang, and G. K. Karagiannis, "Secure multiple amplify-and-forward relaying over correlated fading channels," *IEEE Transactions on Commun.* **65**, 2811–2820 (2017).
  34. J. Zhang, X. Li, I. S. Ansari, Y. Liu, and K. A. Qaraqe, "Performance analysis of dual-hop DF satellite relaying over  $\kappa$ - $\mu$  shadowed fading channels," in *2017 IEEE Wireless Communications and Networking Conference (WCNC)*, (IEEE, 2017), pp. 1–6.
  35. M. Arti, "Beamforming and combining based scheme over  $\kappa$ - $\mu$  shadowed fading satellite channels," *IET Commun.* **10**, 2001–2009 (2016).
  36. Y. Zou, J. Zhu, X. Li, and L. Hanzo, "Relay selection for wireless communications against eavesdropping: A security-reliability trade-off perspective," *IEEE Netw.* **30**, 74–79 (2016).
  37. A. P. Shrestha, J. Jung, and K. S. Kwak, "Secure wireless multicasting in presence of multiple eavesdroppers," in *2013 13th International Symposium on Communications and Information Technologies (ISCIT)*, (IEEE, 2013), pp. 814–817.
  38. D. K. Sarker, M. Z. I. Sarker, and M. S. Anower, "Secure wireless multicasting through AF-cooperative networks with best-relay selection over generalized fading channels," *Wirel. Networks* pp. 1–14 (2018).
  39. D. Sarker, M. Sarkar, and M. Anower, "Secure wireless multicasting with linear equalization," *Phys. Commun.* **25**, 201–213 (2017).
  40. X. Wang, M. Tao, and Y. Xu, "Outage analysis of cooperative secrecy multicast transmission," *IEEE Wirel. Commun. Lett.* **3**, 161–164 (2014).
  41. M. Srinivasan and S. Kalyani, "Secrecy capacity of  $\kappa$ - $\mu$  shadowed fading channels," *IEEE Commun. Lett.* **22**, 1728–1731 (2018).
  42. S. Al-Juboori and X. N. Fernando, "Multiantenna Spectrum Sensing Over Correlated Nakagami-m Channels with MRC and EGC Diversity Receptions," *IEEE Transactions on Veh. Technol.* **67**, 2155–2164 (2017).
  43. R. D. Yates and D. J. Goodman, *Probability and Stochastic Processes: a Friendly Introduction for Electrical and Computer Engineers* (John Wiley & Sons, 2014).

44. N. Kumar and V. Bhatia, "Performance Analysis of Amplify-and-Forward Cooperative Networks with Best-Relay Selection Over Weibull Fading Channels," *Wirel. Pers. Commun.* **85**, 641–653 (2015).
45. M. Ibrahim, A. Badrudduza, M. Hossen, M. K. Kundu, I. S. Ansari *et al.*, "Enhancing security of TAS/MRC based mixed RF-UOWC system with induced underwater turbulence effect," *arXiv preprint arXiv:2105.09088* (2021).
46. M. K. Simon and M.-S. Alouini, *Digital Communication over Fading Channels*, vol. 95 (John Wiley & Sons, 2005).
47. I. S. Gradshteyn and I. M. Ryzhik, *Table of Integrals, Series, and Products* (Academic, San Diego, CA, 2007), 7th ed.
48. I. Krikidis, J. S. Thompson, S. McLaughlin, and N. Goertz, "Max-Min Relay Selection for Legacy Amplify-and-Forward Systems with Interference," *IEEE Transactions on Wirel. Commun.* **8**, 3016–3027 (2009).
49. J. P. Pena-Martin, J. M. Romero-Jerez, and C. Tellez-Labao, "Performance of selection combining diversity in  $\eta$ - $\mu$  fading channels with integer values of  $\mu$ ," *IEEE Transactions on Veh. Technol.* **64**, 834–839 (2014).
50. S. H. Islam, A. S. M. Badrudduza, S. M. Riazul Islam, F. I. Shahid, I. S. Ansari, M. K. Kundu, S. K. Ghosh, M. B. Hossain, A. S. M. S. Hosen, and G. H. Cho, "On secrecy performance of mixed Generalized Gamma and Málaga RF-FSO variable gain relaying channel," *IEEE Access* **8**, 104127–104138 (2020).
51. N. H. Juel, A. Badrudduza, S. R. Islam, S. H. Islam, M. kumar Kundu, I. S. Ansari, M. M. Mowla, and K.-S. Kwak, "Secrecy performance analysis of mixed  $\alpha$ - $\mu$  and Exponentiated Weibull RF-FSO cooperative relaying system," *IEEE Access* (2021).
52. K. An, T. Liang, X. Yan, and G. Zheng, "On the Secrecy Performance of Land Mobile Satellite Communication Systems," *IEEE Access* **6**, 39606–39620 (2018).
53. N. A. Sarker, A. S. M. Badrudduza, S. M. R. Islam, S. H. Islam, I. S. Ansari, M. K. Kundu, M. F. Samad, M. B. Hossain, and H. Yu, "Secrecy performance analysis of mixed Hyper-Gamma and Gamma-Gamma cooperative relaying system," *IEEE Access* **8**, 131273–131285 (2020).
54. S. H. Islam, A. Badrudduza, S. R. Islam, F. I. Shahid, I. S. Ansari, M. K. Kundu, and H. Yu, "Impact of correlation and pointing error on secure outage performance over arbitrary correlated Nakagami- $m$  and  $M$ -turbulent fading mixed RF-FSO channel," *IEEE Photonics J.* **13**, 1–17 (2021).
55. V. Bankey and P. K. Upadhyay, "Physical Layer Security of Multiuser Multirelay Hybrid Satellite-Terrestrial Relay Networks," *IEEE Transactions on Veh. Technol.* **68**, 2488–2501 (2019).
56. W. Liu, Z. Ding, T. Ratnarajah, and J. Xue, "On ergodic secrecy capacity of random wireless networks with protected zones," *IEEE Transactions on Veh. Technol.* **65**, 6146–6158 (2015).
57. K. Guo, K. An, B. Zhang, Y. Huang, and D. Guo, "Physical Layer Security for Hybrid Satellite Terrestrial Relay Networks With Joint Relay Selection and User Scheduling," *IEEE Access* **6**, 55815–55827 (2018).
58. A. S. M. Badrudduza, M. Ibrahim, S. M. R. Islam, M. S. Hossen, M. K. Kundu, I. S. Ansari, and H. Yu, "Security at the physical layer over GG fading and mEGG turbulence induced RF-UOWC mixed system," *IEEE Access* **9**, 18123–18136 (2021).
59. J. Sun, X. Li, Y. Ding, and J. Du, "On physical layer security over SIMO  $\kappa$ - $\mu$  shadowed fading channels," *Recent Adv. Electr. Electron. Eng.* (2019).
60. N. Bhargav, S. L. Cotton, and D. E. Simmons, "Secrecy Capacity Analysis Over  $\kappa$ - $\mu$  Fading Channels: Theory and Applications," *IEEE Transactions on Commun.* **64**, 3011–3024 (2016).
61. N. A. Sarker, A. S. M. Badrudduza, M. K. Kundu, and I. S. Ansari, "Effects of eavesdropper on the performance of mixed  $\eta$ - $\mu$  and DGG cooperative relaying system," *arXiv preprint arXiv:2106.06951v1* (2021).
62. N. S. Mandira, M. K. Kundu, S. H. Islam, A. Badrudduza, and I. S. Ansari, "On secrecy performance of mixed  $\alpha$ - $\eta$ - $\mu$  and Málaga RF-FSO variable gain relaying channel," *arXiv preprint arXiv:2105.12265* (2021).